

VISUALIZATION OF CADHERIN-CADHERIN ASSOCIATION
IN LIVING CELLS

Thesis by

Eric Mosser

In Partial Fulfillment of the Requirements

For the Degree of

Doctor of Philosophy

California Institute of Technology

Pasadena, California

2007

(Defended November 30, 2006)

© 2007

Eric Mosser

All Rights Reserved

ACKNOWLEDGEMENTS

I would like to first thank Dr. Erin Schuman, whose laboratory this work was conducted in. Without her guidance and determination, I probably would have dropped this project after several years without success. I am grateful for her insight and advice along the way, as well as her critical eye for poetry.

I would also like to thank my committee members; Scott Fraser, Pamela Bjorkman, and Kai Zinn, for assistance throughout my graduate school career. They have all been a sounding board for ideas and a source of the same.

I would also like to thank the members (past and current) of the Schuman lab, especially Chin-Yin Tai for her help with the work described here and her endless cheer, and Sachiko Murase for her help in getting me started and up-to-speed on cadherins. Sachiko helped to teach me most of the techniques described in this work.

I would also like to thank my family, who has always been nothing but supportive and understanding of pretty much every endeavor I've decided on. Without them I wouldn't have gotten to where I am today.

ABSTRACT

The almost universally accepted model for long-term potentiation (LTP) involves Ca^{2+} flux through NMDA receptors into dendritic spines. This Ca^{2+} influx may cause a transient Ca^{2+} decrease in the synaptic cleft. We hypothesize that this decrease in cleft Ca^{2+} may destabilize cadherin-cadherin bonds in the synapse and that this conformational change may allow synaptic cadherins to function as synaptic activity sensors.

In the last decade, much effort has been devoted to understanding the structure and molecular associations of classic cadherins. Crystallographic and biophysical studies have yielded somewhat conflicting results and an as yet unclear picture of the homotypic interactions of the cadherin extracellular domain during dimerization. To better understand the dynamics of cadherin interactions we have developed Fluorescence Resonance Energy Transfer (FRET) based sensors to monitor cadherin associations across cellular junctions in a dynamic manner in living cells.

Here, we demonstrate the functionality of FRET-based cadherin interaction reporters. FRET is unique in its ability to provide signals that are sensitive to changes in intra- or intermolecular distances in the 1-10 nm range, well below the inherent diffraction limit of conventional fluorescence microscopy. We believe that FRET is a powerful technique to monitor cadherin orientation and interactions in heterologous, living cells.

TABLE OF CONTENTS

ACKNOWLEDGEMENTS.....	iii
ABSTRACT.....	iv
TABLE OF CONTENTS.....	v
LIST OF ILLUSTRATIONS.....	vii
ABBREVIATIONS USED.....	viii
Chapter I.....	1
INTRODUCTION.....	1
Synaptic plasticity – functional and structural.....	2
Adhesion molecules at the synapse.....	2
Chapter II.....	4
LITERATURE REVIEW.....	4
Cadherins.....	5
<i>Cadherin structure and adhesive function</i>	7
<i>Neuronal cadherins</i>	9
β -Catenin.....	12
Synaptic plasticity.....	15
The importance of Ca^{2+} ion.....	17
<i>Cadherins and Ca^{2+}</i>	17
<i>Ca^{2+} in the extracellular space</i>	18
<i>Ca^{2+} and LTP</i>	19
FRET as a tool for studying protein dynamics.....	20
Chapter III.....	22
ANALYSIS OF β -CATENIN DYNAMICS IN NEURONS.....	22
Chapter IV.....	28
DEVELOPMENT OF CADHERIN FRET REPORTERS.....	28
<i>Epitope tagging approaches</i>	29
<i>Fluorescent protein approaches</i>	31
<i>Transposon-mediated functional insertion of fluorescent proteins in N-cadherin</i> ... 32	
<i>Monitoring cadherin interactions via acceptor bleaching (adFRET)</i>	38
<i>Visualizing changes in cadherin-cadherin interactions induced by changes in extracellular Ca^{2+} concentration</i>	43
Chapter V.....	49
DISCUSSION AND FUTURE DIRECTIONS.....	49
<i>Construction of cadherin FRET reporters</i>	50
<i>Geometry of cadherins in cell junctions</i>	52
<i>Visualizing changes in cadherin-cadherin interactions induced by synaptic activity</i>	54
<i>Experiments made possible with cadherin FRET reporters</i>	58
WORK CITED.....	62
APPENDIX.....	69
MATERIALS AND METHODS.....	69
<i>Constructs, viruses and antibodies</i>	69
<i>Cultured hippocampal neurons</i>	69
<i>Cell culture and transfection</i>	70

<i>Immunoprecipitation</i>	70
<i>L cell aggregation assay</i>	71
<i>Microscopy and image analysis</i>	72

LIST OF ILLUSTRATIONS

Figure 1. Schematic diagram of the molecular structure of the cadherin superfamily and their cytoplasmically associated proteins.....	6
Figure 2. Mutation of a β -catenin tyrosine residue affects the size and intensity of presynaptic and postsynaptic protein clusters.....	25
Figure 3. Scheme of β -catenin's redistribution following synaptic activity or mutation of tyrosine 654.....	27
Figure 4. Structure of the N-terminal EC domain (EC1) of E-cadherin.....	30
Figure 5. Overview of the bacterial transposon-mediated random insertion.....	34
Figure 6. Functional assays of GFP-N-cadherin fusion proteins.....	37
Figure 7. Overview of FRET and the acceptor bleach FRET experiment.....	38
Figure 8. adFRET in HEK-293 cells expressing both CFP-N-cadherin and YFP-N-cadherin revealing cadherin <i>cis</i> interactions.....	40
Figure 9. adFRET at cell junctions between COS7 cells separately expressing Cerulean-N-cadherin or Venus-N-cadherin.....	42
Figure 10. Monitoring changes in FRET induced by changes in extracellular Ca^{2+} concentration in COS7 cells.....	44
Figure 11. Monitoring changes in FRET induced by changes in extracellular Ca^{2+} concentration in COS7 cells.....	47
Figure 12. Quasi-to-scale schematic of fully interdigitated ectodomain model of cadherin interactions.....	53
Figure 13. A hippocampal neuron expressing Venus-cadherin.....	55

ABBREVIATIONS USED

adFRET	acceptor depletion FRET
AMPA	alpha-amino-3-hydroxy-5-methyl-4-isoxazolepropionic acid
APV	R-2-amino-5-phosphonopentanoate
BDNF	brain derived neurotrophic factor
CA1	cornu ammonis field 1
Cdk5	cyclin-dependent kinase 5
CHO	Chinese hamster ovary
CNQX	6-cyano-7-nitroquinoxaline-2,3-dione
COS7	a cell line of transformed monkey kidney cells
DIV	days <i>in vitro</i>
DNA	deoxyribonucleic acid
EC	extracellular cadherin repeat
Ecad	E-cadherin
ECFP	enhanced cyan fluorescent protein
EGFP	enhanced green fluorescent protein
EGTA	ethylene glycol tetraacetic acid
EM	electron microscopy
EPSC	excitatory postsynaptic current
ER	endoplasmic reticulum
EYFP	enhanced yellow fluorescent protein
FRET	fluorescence (or Förster) resonance energy transfer
GABA	gamma-amino-butyric acid

HA	hemagglutinin
HAV	histidine alanine valine
HBS	HEPES-buffered saline
HEK293	a human embryonic kidney cell line
KCl	potassium chloride
LSM	laser scanning microscope
LTP	long term potentiation
Ncad	N-cadherin
NMDA	N-methyl-D-aspartic acid
NMDAR	NMDA receptor
NMR	nuclear magnetic resonance
p120	p120 catenin
PA	puncta adherentia
PBS	phosphate buffered saline
PCR	polymerase chain reaction
PKA	protein kinase A
PSD	postsynaptic density
ROI	region of interest
Trp	tryptophan
TTX	tetrodotoxin
XFP	EGFP variant (nonspecific)
Zeo	zeomycin

Chapter I
INTRODUCTION

Synaptic plasticity – functional and structural

Brain function is mediated by highly specific circuits that connect widely separate groupings of neurons into functional networks. Such precision in organization is established during development, as connections are made to yield a mature framework for brain function. After development, synaptic connectivity remains functionally dynamic throughout life, allowing new associations appropriate for learning and memory formation, and for repair in case of injury. An important area of neurobiological research focuses on understanding how synapses are formed, maintained, and modified to allow such behavioral flexibility (plasticity).

Synaptic plasticity is the ability of the connections between neurons to change in strength. Plasticity can involve (1) a structural change in synapses (changes in synapse size, formation of new synapses, or elimination of existing ones, or changes in the shape or geometry of spines); (2) changes in the molecular composition of existing synapses (addition of new molecular species or changes in the numbers of the different molecules in the synapse); or (3) changes in the state of the existing molecules of the synapse (changes in phosphorylation state, or other posttranslational modifications).

Adhesion molecules at the synapse

Adhesion molecules are membrane-anchored molecules whose extracellular domains directly interact to help hold the membranes of two cells together. Maintenance of an apposition of the two membranes can be the primary role of the interaction or can result secondarily because of ligand-receptor interactions whose primary purpose is to transmit signals to the cytoplasm.

Adhesion molecules are involved in the regulation of synaptic structure and function. Such involvement is of importance both to synapse maturation, which requires the elaboration of presynaptic boutons and postsynaptic spines, and to synaptic plasticity. Several adhesion molecules are known to regulate spine morphology, as well as electrophysiological measures of the strength of existing synapses which results from nonstructural changes (2) and (3) above). One such example is the cadherins, a group of calcium dependent homophilic adhesion proteins.

In the following chapters, I will first discuss work that has been done describing cadherins, their structure and function, and their role in the nervous system. Second, I will describe my work on developing FRET-based reporters of cadherin adhesive state. Last, I describe my use of these reporters in studying the response of cadherin homophilic interactions to changes in extracellular calcium ion concentration.

Chapter II
LITERATURE REVIEW

Cadherins

The cadherins are a large superfamily of calcium-dependent cell adhesion proteins. The cadherin superfamily includes classic cadherins, desmosomal cadherins, protocadherins, and other cadherin-related proteins, all of which have multiple repeats of an approximately 110 amino acid cadherin-specific motif (the extracellular cadherin repeat, or EC), in their extracellular domain (figure 1) (reviewed in Angst and Marcozzi, 2001; Takeichi and Abe 2005; Suzuki 1996). The classic cadherins, of which there are ~20, were the first discovered and are the best studied. Examples of classic cadherins include neural (N)-, retinal (R)-, vascular endothelial (VE)-, epithelial (E)-, and placental (P)-cadherin, named by the tissues in which they were originally discovered, but now known to have much broader tissue distributions. Classic cadherins are characterized by a highly conserved C-terminal cytoplasmic domain, a single transmembrane domain, and an N-terminal ectodomain consisting of five EC repeats. Calcium ions, which are required for adhesive binding, intercalate between the EC domains to produce a rigidified, rodlike ectodomain (Nagar, Overduin et al. 1996).

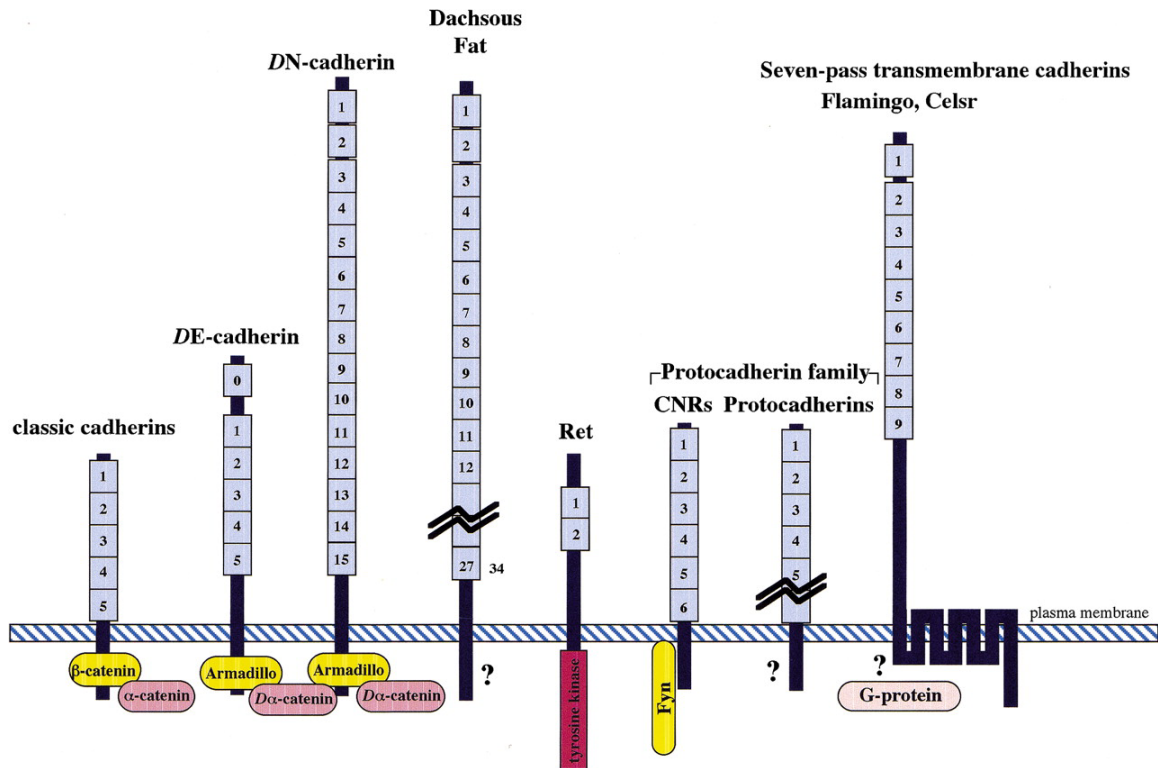


Figure 1. Schematic diagram of the molecular structure of the cadherin superfamily (blue) and their cytoplasmically associated proteins (yellow, pink) (from Yagi and Takeichi 2000).

Intracellularly, classic cadherins associate with a number of different kinds of molecules that mediate downstream signaling, as well as the actin cytoskeleton. The catenins (α , β , and γ) link classic cadherins to the actin cytoskeleton; this linkage is essential for adhesive function (Nagafuchi and Takeichi 1988). Interactions with other intracellular proteins such as p120, δ -catenin, and presenilin are thought to regulate dimerization of cadherins expressed in the membrane of the same cell (as known as *cis* interactions, discussed in the next section below). This has been shown to modulate the strength of interactions with cadherins on adjacent cells (known as *trans* interactions)

presumably by laterally clustering cadherins on the cell surface (Yap, Niessen et al. 1998; Baki, Marambaud et al. 2001).

Cadherin structure and adhesive function

Initial structural studies of cadherins (Shapiro, Fannon et al. 1995; Overduin, Harvey et al. 1995) utilized X-ray crystallography and NMR spectroscopy to determine the structure of the most N-terminal (most distal from the cell membrane) EC repeat, as this repeat was known from earlier work to be necessary for homophilic binding specificity (Nose, Tsuji et al. 1990). This work showed the EC structure to consist of 7 β strands and 2 α helices in a β -barrel topology similar to the immunoglobulin fold. Earlier studies had demonstrated that a conserved amino acid sequence, the HAV region (residues 79–81 of E-cadherin), which is common to the first EC of all cadherins, was required for adhesive function (Blaschuk, Sullivan et al. 1990). The surface displaying this HAV sequence, as well as the residues responsible for Ca^{2+} ion binding, were also determined.

Based on crystal lattice contacts observed in the structure of the first EC repeat, a two-step cadherin association mechanism was proposed (Shapiro, Fannon et al. 1995). First, a *cis* interaction pair (that was dubbed the “strand dimer”) is formed between two parallel molecules by mutual exchange of a β -strand due to binding of a tryptophan (Trp2) from one molecule into a hydrophobic pocket of the partner molecule. Second, a *cis* dimerized pair undergoes a *trans* interaction (dubbed the “adhesion dimer”) with a complementary antiparallel unit. Alternating *cis* and *trans* interactions then form a zipperlike superstructure.

These initial structural studies implicate only the first 2 ECs in these interactions. Several later studies, including a crystallization of the entire extracellular domain of C-cadherin (Boggon, 2002) and an electron tomographic study of epithelial desmosomes (He, Cowin et al. 2003) in which this C-cadherin ectodomain structure was fit to electron densities, representing cadherins in their “in situ habitat”, confirmed the involvement of only the first 2 ECs. In contrast to the crystallographic studies, the tomography showed a much less ordered packing of cadherins, with the cadherin N-terminal interactions not forming a regular lattice. Cadherins were seen to assemble into groups of 10 to 20 molecules, with their N-terminal domains forming a series of “knots” at the midline of the cell-cell junction. Similar to the latticed packing seen in crystals, this grouping facilitates extensive interactions between EC domains.

In contrast to this N-terminal model for cadherin interactions, a number of biophysical studies have, through the use of surface force probes (Perret, Leung et al. 2004; Sivasankar, Gumbiner et al. 2001; Zhu, Chappuis-Flament et al. 2003) and cadherin-coated beads in a flow chamber (Perret, Benoliel et al. 2002), suggested that all ECs contribute to the interactions and interestingly, the strongest interaction is detected when all ECs are bound to each other (Perret, Leung et al. 2004), with the cadherin ectodomains fully interdigitated.

Functional inactivation of E-cadherin in CHO cells by mutating several conserved cysteine residues in EC5, the EC closest to the plasma membrane, further supports the idea that all ECs contribute to the interaction (Chappuis-Flament, Wong et al. 2001). Taking all of this data together, it appears that the most distal ECs (1 and 2)

are likely the most important for homophilic interactions, but the other ECs (3-5) also participate.

Cadherin-mediated adhesion generates stable, tight junctions. In adults, interactions between cadherins on adjacent cells help to maintain the structural integrity of solid tissues and regulate the turnover and reorganization of tissue structures. For example, in adherens junctions between epithelial cells, E-cadherin forms the transport barrier between the intestine and bloodstream, while vascular endothelial cadherin (VE-cadherin) maintains the barrier properties of blood vessels. In addition to being stable enough to maintain tissue integrity, these junctions must be sufficiently plastic to permit rapid remodeling of tissue interfaces, allow for cell motility, and enable cellular rearrangements during different stages in development.

Understanding how cadherins form cell-cell junctions is central to understanding their role in biology. A fundamental challenge is to determine the mechanism of intercellular adhesive bond formation.

Neuronal cadherins

Cadherins are expressed in many tissues, including the central nervous system where they are most well known for their role in target recognition and stabilization during synaptogenesis. Crucial to synaptogenesis is the ability of axons to grow to their targets and form synapses with the correct postsynaptic cell type. Axons often travel long distances before reaching their final target, and although they come in contact with many potential partners along the way, they do not establish synapses on inappropriate cells.

Given the large number of targets, the system (or systems) mediating this recognition would need to be complex, and this requirement could only be met by adhesion proteins that offer sufficient combinatorial possibilities. This “lock and key” mechanism was first hypothesized by Sperry in 1963, and implies the existence of specific adhesion molecules that pair axons with their targets. There are now known to be at least 80 cadherins likely to be expressed in nervous tissue, including the classical cadherins and the protocadherins; this positions cadherins as likely candidates for a role as “synaptic specifiers.”

There are many lines of evidence to support the idea that cadherins are responsible for proper synapse formation: Blockade of N-cadherin function in cultured hippocampal neurons by overexpression of a dominant negative cadherin (which lacks its ectodomain) results in a significant block of synapse assembly, detected as a loss of spines and an increase in the number of filopodia (Togashi, Abe et al. 2002). These effects are more pronounced in younger neurons, demonstrating that cadherins are active at earlier stages of synapse development. In addition, synapses that form on neurons that overexpress the dominant negative cadherin are smaller than controls and have decreased synaptic vesicle recycling and a decreased frequency of spontaneous EPSCs. They also fail to acquire resistance to F-actin depolymerization, which is a hallmark of mature, stable synapses. (Bozdagi, Valcin et al. 2004).

In the retinotectal system, treatment with antibodies that block N-cadherin adhesion causes retinal ganglion cells to overshoot their targets (Inoue and Sanes 1997). In the cerebellum, cadherins have been shown to appear in distinct cortical “stripes,”

expressed in cells that project to underlying nuclei expressing the same cadherin, forming zones of topographically organized connections (Arndt, Nakagawa et al. 1998).

N-cadherin has been proposed to mediate the initial synaptic adhesion of the thalamocortical projections from the ventrobasal nucleus (that represent the facial vibrissae, or “whiskers”) to the barrel field of somatosensory cortex. Levels of N-cadherin in thalamic axons decrease at postnatal day 9, however, α N- and β -catenin persist at the adult synapse (Huntley and Benson 1999). In hippocampal cultures N-cadherin first appears at all synapses but rapidly disappears in all but excitatory glutamatergic synapses (Benson and Tanaka 1998). In these last two studies, the persistence of β -catenin at synapses at which N-cadherin is eventually not present suggests that other cadherins may become important at these synapses during the course of maturation. This indicates that N-cadherin adhesion may stabilize early synapses that can then be remodeled and express a different cadherin.

These studies demonstrate the diverse roles of cadherins in synaptogenesis, and taken together, show cadherins to be deeply involved in regulation of axonal target specificity.

Cadherin neuronal expression however, persists into adulthood, arguing for a cadherin role beyond synapse formation. In 1995, it was demonstrated by a combination of immunoprecipitation and Western blot analyses that N-cadherin is a major constituent of isolated rat forebrain postsynaptic densities (Beesley, Mummery et al. 1995). A subsequent study used confocal microscopy to optically section through synaptic junctions in adult mouse cerebellum, and, by rotating the stacked images, showed that in many cases, N-cadherin immunolabeling formed a ring that surrounded a central “pore”

of the presynaptic protein synaptophysin (Fannon and Colman 1996). α N and β -catenin have been shown to be localized to apposed pre- and postsynaptic membranes in circumscribed zones that flank the active zone presynaptically, the site of vesicle release, and the postsynaptic density, in which the neurotransmitter receptors are localized (Uchida, Honjo et al. 1996). Reconstruction from serial electron microscopy was used to determine the location and size of puncta adherens (cell junctions with enriched levels of adhesion molecules, including cadherins) in the stratum radiatum of hippocampal area CA1: puncta adherens were found at the edges of synapses on 33% of dendritic spines (Spacek and Harris 1998).

A number of more recent studies have used confocal microscopy to examine the distribution of various cadherins in relationship to immunolabeling for synaptic vesicle proteins such as synaptophysin (Arndt, Nakagawa et al. 1998; Benson and Tanaka 1998; Tang, Hung et al. 1998).

β -Catenin

As discussed above, β -catenin binds to the intracellular domain of cadherin and links it to the actin cytoskeleton through β -catenin's interaction with α -catenin, a vinculin-like actin-binding protein. This linkage is required for cadherin adhesive function – when cadherin with a deleted β -catenin binding site is expressed in L cells (a cell line lacking endogenous cadherins but expressing all catenins), the extracellular domain of the mutant E-cadherins was properly exposed on the cell surface, and had normal Ca^{2+} -sensitivity and molecular size. However, L cells expressing these mutant cadherins did not show any Ca^{2+} -dependent aggregation, indicating that the mutant molecules cannot mediate cell-cell binding (Nagafuchi and Takeichi 1988).

β -catenin interaction with cadherins is known to be negatively regulated by tyrosine phosphorylation (Roura, Miravet et al. 1999; Muller, Choidas et al. 1999; Pathre, Arregui et al. 2001; Sommers, Gelmann et al. 1994). Cyclin-dependent kinase 5 (Cdk5)/p35 kinase has been implicated as the responsible kinase, through its effect on the phosphorylation level of tyrosine-654 of β -catenin (Schuman and Murase 2003).

Our laboratory has shown that tyrosine kinase inhibitor promoted redistribution of β -catenin into spines, suggesting that under normal conditions, constitutive phosphorylation of β -catenin reserves substantial levels of β -catenin in the dendritic shaft (Murase et al., 2002). Consistent with this, postsynaptic expression of a mutant β -catenin in which phosphorylation was prevented resulted in its accumulation at spines. In contrast, expression of a phosphorylation-mimic mutant accumulated in the dendrite shafts. Accumulation of the dephosphorylation-mimic β -catenin mutant in spines was accompanied by an increase in the size of synapsin and PSD-95 clusters. Furthermore, presynaptic activity was elevated, as judged by an increase in FM4-64 dye uptake and the rate of spontaneous neurotransmitter release. We also showed that β -catenin moves from dendritic shafts into spines upon depolarization, increasing its association with cadherins ((Murase, Mosser et al. 2002) - my contributions to this work are discussed in chapter III). As a corollary to this, Togashi et al. observed that synapsin and PSD-95 puncta as well as FM4-64 dye uptake were decreased when spine localization of β -catenin was impaired by expression of a dominant-negative N-cadherin lacking a portion of the extracellular domain (Togashi, Abe et al. 2002).

In 2003, Bamji et al., used EM analysis to show a reduction in the number of synaptic vesicles in the neurons of β -catenin conditional knockout mice. Recently, the same group showed that brain derived neurotrophic factor (BDNF) mobilizes synaptic vesicles at existing synapses, causing small clusters of synaptic vesicles to "split" away from synaptic sites. This ability of BDNF to mobilize synaptic vesicle clusters depends on the dissociation of cadherin- β -catenin adhesion complexes that occurs after tyrosine phosphorylation of β -catenin. Overexpression of the phosphorylation-blocked mutant β -catenin increases cadherin- β -catenin interactions and abolishes the BDNF-mediated enhancement of synaptic vesicle mobility, as well as the longer-term BDNF-mediated increase in synapse number (Bamji, Rico et al. 2006).

In addition to its role in linking cadherin to the actin cytoskeleton, β -catenin has long been known for the part it plays through the Wnt signaling pathway, in tumorigenesis. Cell-cell interactions are known to be a factor in cancer, and it has been suggested that β -catenin may be a key player in linking cell adhesion to transcriptional signaling through the Wnt pathway. Control of these dual functions is crucial for maintaining normal cellular function. Deregulation, which promotes the transcriptional function of β -catenin over its function in adhesion, is a major factor in the development and progression of many human malignancies (reviewed in Brembeck, Rosario et al. 2006).

It is clear that cadherins and their associated proteins, such as the catenins, play an important role in coordinating surface adhesion and cell recognition with cytoskeletal activity and cell signaling.

Synaptic plasticity

Although initial views of cadherin function in the nervous system were dominated by cadherin's roles in establishing brain structure and synaptic connectivity during development, their function at the synapse involves more than a merely structural role and includes a capability for modulation of the synaptic signal itself.

The phrase "synaptic plasticity" is used to describe changes in the strength of a synaptic signal as recorded electrophysiologically, as well as changes in synapse morphology or number. These two different forms of plasticity (functional vs. structural) are thought to be related as changes in synapse structure or number are thought to contribute to functional changes in synaptic strength. There is evidence for a cadherin role in both of these forms of plasticity. Cadherins have been studied, in this regard, mostly in the context of hippocampal long-term potentiation (LTP). LTP is characterized by an increase in synaptic strength lasting from several hours to days or longer, and is the primary cellular model for how neurons enable learning and memory formation (first described in Anderson and Lomo 1966; Bliss and Lomo 1973). In hippocampal area CA1, LTP shows two distinct phases: an early phase (E-LTP) that does not require protein synthesis and lasts ~1 to 2 h, and is thought to reflect posttranslational modifications and translocation of pre- and postsynaptic proteins (reviewed in Nicoll, 1999); and a more slowly developing, but long-lasting late phase (L-LTP) that requires gene transcription and protein synthesis and lasts many hours to days or longer (reviewed by Bailey, Bartsch et al. 1996). This phase may also reflect synaptic structural changes. Induction of late-phase LTP in hippocampal area CA1 appears to cause the growth of new dendritic spines or filopodia (suggested to serve as spine precursors (reviewed in

Yuste and Bonhoeffer 2004)) on the dendrites postsynaptic to the stimulated synapses (Engert and Bonhoeffer 1999; Maletic-Savatic, Malinow et al. 1999). LTP induction has also been found to result in ultrastructural modifications to existing synapses, with apparent increases in the number of perforated synapses, the size of the apposition zones between pre-and postsynaptic structures, and the length of the PSD (Buchs and Muller 1996). As discussed, this sort of structural remodeling brings with it a requirement for a stable, yet plastic means of regulating cellular adhesion. As mentioned above, cadherins have been shown to have a role in both functional and structural plasticity.

Induction of late-phase LTP has been shown to cause a significant increase in the number of synaptic puncta identified by visualizing synaptophysin and N-cadherin. This increase was PKA- and protein synthesis dependent. This induction also caused an increase in N-cadherin dimerization indicating a specific role for N-cadherin in the signal transduction cascade that leads to lasting synaptic potentiation (Bozdagi, Shan et al. 2000).

When cultured hippocampal cells are stimulated using high K^+ to depolarize them, N-cadherin dimerizes and acquires a long-lasting protease resistance (Tanaka, Shan et al. 2000). This has been shown to be protein synthesis independent and is not accompanied by N-cadherin internalization. In addition, N-cadherin, normally localized in discrete puncta in close proximity to the PSD, is rapidly and actively dispersed laterally along the plasma membrane upon depolarization with high K^+ . Furthermore, the presence of the NMDA receptor antagonist APV attenuated this acquisition of protease resistance and dimerization while direct stimulation with NMDA induced a high level of protease resistance and dimerization but does not induce cadherin dispersion.

The importance of Ca^{2+} ion

Cadherins and Ca^{2+}

Cadherin adhesion has a strict requirement for calcium, which rigidifies the interrepeat links and apparently activates *trans* interactions (Hyafil, Babinet et al. 1981). In the absence of calcium, cadherins undergo a reversible loss of their rodlike structure and collapse (Pokutta, Herrenknecht et al. 1994). Electron microscopic studies of oligomerized E-cadherin extracellular domains at different calcium concentrations have revealed that relatively low calcium concentrations ($\geq 50 \mu\text{M}$) are required to maintain the overall rodlike structure of the ectodomain, while higher concentrations ($\geq 500 \mu\text{M}$) are required for *cis* interactions (Pertz, Bozic et al. 1999). Ca^{2+} ions bind to pockets in the interrepeat regions of the cadherin extracellular domain with a stoichiometry of 3 Ca^{2+} per calcium-binding domain (Nagar, Overduin et al. 1996; Tamura, Shan et al. 1998). Interestingly, these sites bind Ca^{2+} with different affinities; when considered as an intact structure, the complete extracellular region binds Ca^{2+} with an average dissociation constant (K_d) of $30 \mu\text{M}$ (Koch, Pokutta et al. 1997), consistent with the minimal calcium concentrations required to maintain cadherin structure. The 3 Ca^{2+} binding sites between the two most N-terminal domains (EC1 and 2) were found to have K_d s at least an order of magnitude higher. One site of these 3, in particular, was shown to have a particularly high K_d (2 mM, as opposed to $330 \mu\text{M}$ for the other 2), implicating its role in the *trans* interactions only seen at higher calcium concentrations ($>1 \text{ mM}$) (Pertz, Bozic et al. 1999).

Ca²⁺ in the extracellular space

It is interesting to consider the Ca²⁺ dependence of cadherin interactions in the context of the physiological concentrations of calcium found in the extracellular space in neurons. Average extracellular Ca²⁺ concentrations in mammalian brain range from 1.5 to 2.0 mM (Jones and Heinemann 1987), which is well within the range where cadherins engage in both *cis* and *trans* interactions. Experimental techniques have not yet provided direct, rapid measurements of Ca²⁺ concentration within individual synaptic clefts. However, computation approaches have yielded interesting results: simulations of active synaptic clefts (Egelman and Montague 1998, 1999; Wiest, Eagleman et al. 2000) predict that during synaptic activity, cleft Ca²⁺ concentrations will drop into the range where local synaptic and/or perisynaptic cadherins would lose *trans* interactions (~800 μ M to 1 mM), and possibly (depending on synaptic parameters such as active zone size) to levels that would cause a loss of *cis* interactions as well (~200 μ M). More recently, novel optical methods of measuring extracellular calcium have provided direct measurements of Ca²⁺ concentrations in active neuropil (Rusakov and Fine 2003). These experiments show that brief stimulation evokes significant depletion of extracellular Ca²⁺ in an NMDAR-dependent manner. Since the average synaptic cleft size ($6-8 \times 10^{-4} \mu\text{m}^3$, assuming cleft width of ~20 nm and postsynaptic density area of $0.03 - 0.04 \mu\text{m}^2$) (Rusakov and Kullmann 1998; Schikorski and Stevens 1997; Shepherd and Harris 1998) is below the optical resolution of laser scanning microscopy, direct measurements of Ca²⁺ concentration in the local microenvironment of individual synaptic clefts was not possible, but as the authors point out, the observed ~40-50 μ M decrease in Ca²⁺ over the sampled neuropil volume of ~0.1 μm^3 could be interpreted as almost total depletion of

Ca^{2+} at all active synapse in the area. Thus, experimental data as well as simulations predict that Ca^{2+} is dynamically regulated in the synaptic cleft. This implies that alterations in cleft Ca^{2+} have important ramifications for cadherin-cadherin adhesion and signaling (Murase, Mosser et al. 2002; Tang, Hung et al. 1998).

Ca^{2+} and LTP

LTP and other forms of synaptic plasticity have long been studied as attractive cellular correlates of learning and memory. A widely accepted model for LTP induction involves activation of NMDA receptors, which allows Ca^{2+} to enter the dendritic spine (reviewed in Bliss and Collingridge 1993). The rise in intracellular Ca^{2+} that results is generally agreed upon to be the “trigger” for LTP. As discussed above, Ca^{2+} influx may also result in a Ca^{2+} decrease in the synaptic cleft. This local decrease in Ca^{2+} could cause a loss of cadherin rigidification and disruption of cadherin adhesion.

Treatments that interfere with cadherin function have been shown to significantly attenuate hippocampal LTP. When cadherin adhesion is blocked by either antibodies specific for the N- or E-cadherin ectodomain, or peptides that bind to the conserved HAV sequence discussed above, LTP is inhibited if the peptide or antibody is present during induction of LTP. However, if application of the peptide or antibody is delayed until 30 minutes after LTP induction, no inhibition of LTP occurs (Tang, Hung et al. 1998). The same treatment had no effect on normal synaptic transmission or short-term synaptic plasticity. This suggests that the synaptic activity that leads to induction of LTP may lower local cleft Ca^{2+} concentration and render the synaptic cadherins temporarily vulnerable to antibody or peptide binding. Consistent with this idea, the LTP blocking

effect could be overcome by raising the extracellular Ca^{2+} concentration, presumably compensating for the stimulation induced Ca^{2+} depletion (Tang, Hung et al. 1998). Additionally, during the maintenance phase after successful induction of LTP, extracellular Ca^{2+} was temporarily decreased and then returned to normal levels. When performed in the presence of a scrambled control peptide, LTP recovered to pre- Ca^{2+} -lowering levels. However, when performed in the presence of HAV peptides, this resulted in an inhibition of LTP, with potentiation levels never recovering (Tang and Schuman, unpublished observations).

Thus, HAV peptides inhibit LTP only when applied during induction, or in the presence of reduced extracellular Ca^{2+} . This implies that the inhibition of LTP occurred because the high frequency stimulation used to induce LTP caused a reduction in extracellular Ca^{2+} , disrupting cadherin interactions and allowing the HAV peptides access to their binding sites.

When considered as a whole, current data points strongly to an extracellular Ca^{2+} -mediated role for cadherin in synaptic plasticity.

FRET as a tool for studying protein dynamics

Fluorescence (or Förster) resonance energy transfer (FRET) has been shown to be a useful tool in determining spatiotemporal relationships between molecules (Sorkin, McClure et al. 2000; Broudy, Lin et al. 1998; Damjanovich, Bene et al. 1997; Kenworthy and Edidin 1998; Kenworthy, Petranova et al. 2000; Selvin 1995; Guo, Dower et al. 1995). FRET is a process in which energy is nonradiatively (by means of long-range dipole-dipole coupling) transferred from a donor fluorophore in an electronic excited

state to an acceptor (which may, but does not need to, be fluorescent). The efficiency of energy transfer varies inversely with the 6th power of the donor-acceptor separation over the range of 1-10 nm. This range of distances is relevant for most biomolecules and their subdomains involved in complex formation and conformational changes. Energy transfer by FRET is also dependent on the extent of overlap of donor emission and acceptor adsorption spectra and the relative orientation of the donor and acceptor dipoles. Because of these factors it can be difficult to use FRET to determine absolute distances, but FRET can be quite effectively used to determine relative distances and changes in relative distance.

FRET is unique in its ability to provide signals that are sensitive to changes in intra- or intermolecular distances in the 1-10 nm range, well below the inherent diffraction limit of conventional fluorescence microscopy.

Thus, FRET is an excellent technique to monitor in living cells protein orientation and interactions, allowing us to observe changes in cadherin-cadherin interactions induced by changes in extracellular Ca^{2+} as well as any changes induced by synaptic activity in neurons.

In subsequent chapters, I will first describe my work in analyzing the dynamics of β -catenin in neurons. I will then describe my development of FRET-based cadherin homophilic interaction reporters and their use in studying changes in cadherin interactions in response to extracellular Ca^{2+} concentration.

Chapter III

ANALYSIS OF β -CATENIN DYNAMICS IN NEURONS

As discussed above, I collaborated with Dr. Sachiko Murase, a postdoctoral scholar in the Schuman laboratory to help analyze the dynamics of β -catenin in neurons in response to stimulation (Murase, Mosser et al. 2002). My role in this collaboration was the processing and analysis of the images acquired by Dr. Murase. I was blind to the experimental conditions of each image to ensure a lack of bias in the results of the analysis.

Dr. Murase demonstrated that KCl induced depolarization caused the movement of β -catenin into spines and increased β -catenin/cadherin interactions, as measured by coimmunoprecipitation. Application of tyrosine kinase inhibitor mimicked these effects, while application of a tyrosine phosphatase inhibitor had the opposite effects, indicating that this redistribution of β -catenin was phosphorylation mediated.

The β -catenin phosphorylation mutations (Y654E and Y654F) were sufficient to cause redistribution in a manner consistent with this; the phosphorylation-mimic (Y654E) accumulates in the dendritic shaft, while the dephosphorylation-mimic (Y654F) accumulates in spines.

As noted above, β -catenin's interaction with cadherin is required for cadherin-mediated adhesion. The phosphorylation-mediated movement of β -catenin into spines may promote stabilization and strengthening of cadherin-cadherin interactions, which may be a part of the local expansion of synaptic contacts. To address this issue, we examined the morphological properties of neuronal synapses expressing one of three EGFP- β -catenin fusions; wild-type β -catenin, and two mutants: Y654E, and Y654F. Y654E has tyrosine-654 of β -catenin mutated to glutamic acid; the negative charge of the

glutamate mimics the phosphorylated state of wild-type tyrosine-654. Y654F has its tyrosine-654 mutated to phenylalanine, which has the same aromatic group as tyrosine, but cannot be phosphorylated. This mimics the unphosphorylated state of wild-type tyrosine-654.

To determine whether changes in spine β -catenin concentration result in changes in the size of the postsynaptic density, Dr. Murase fixed the transfected neurons and immunostained them for PSD-95, a prominent component of the postsynaptic density in forebrain neurons (Cho, 1992).

She then captured images, which I was given. I analyzed the images of EGFP signal by selecting the spines, and overlaying the PSD-95 immunostaining images, then identifying the immunostained puncta that overlapped with EGFP labeled spines. I then analyzed the area and intensity of these puncta to determine the effect of mutating tyrosin-654 on PSD clustering.

In Y654F-expressing neurons, the size of the PSD-95 puncta was significantly larger than those of either the Y654E- or wild-type β -catenin-expressing cells, which did not differ significantly from each another (figure 2, B and C). In addition, the intensity of the PSD-95-containing puncta was substantially lower in the Y654E-expressing neurons (figure 2, B and C) and slightly, but significantly, lower in the Y654F-expressing neurons. Thus, the Y654F mutants possessed larger PSD-95 puncta, while the Y654E mutants possessed PSD-95 puncta of the same size, but of lesser intensity.

This suggests that increasing or decreasing the concentration of β -catenin in spines via the point mutation is sufficient to produce changes in the size and “density” of the PSD.

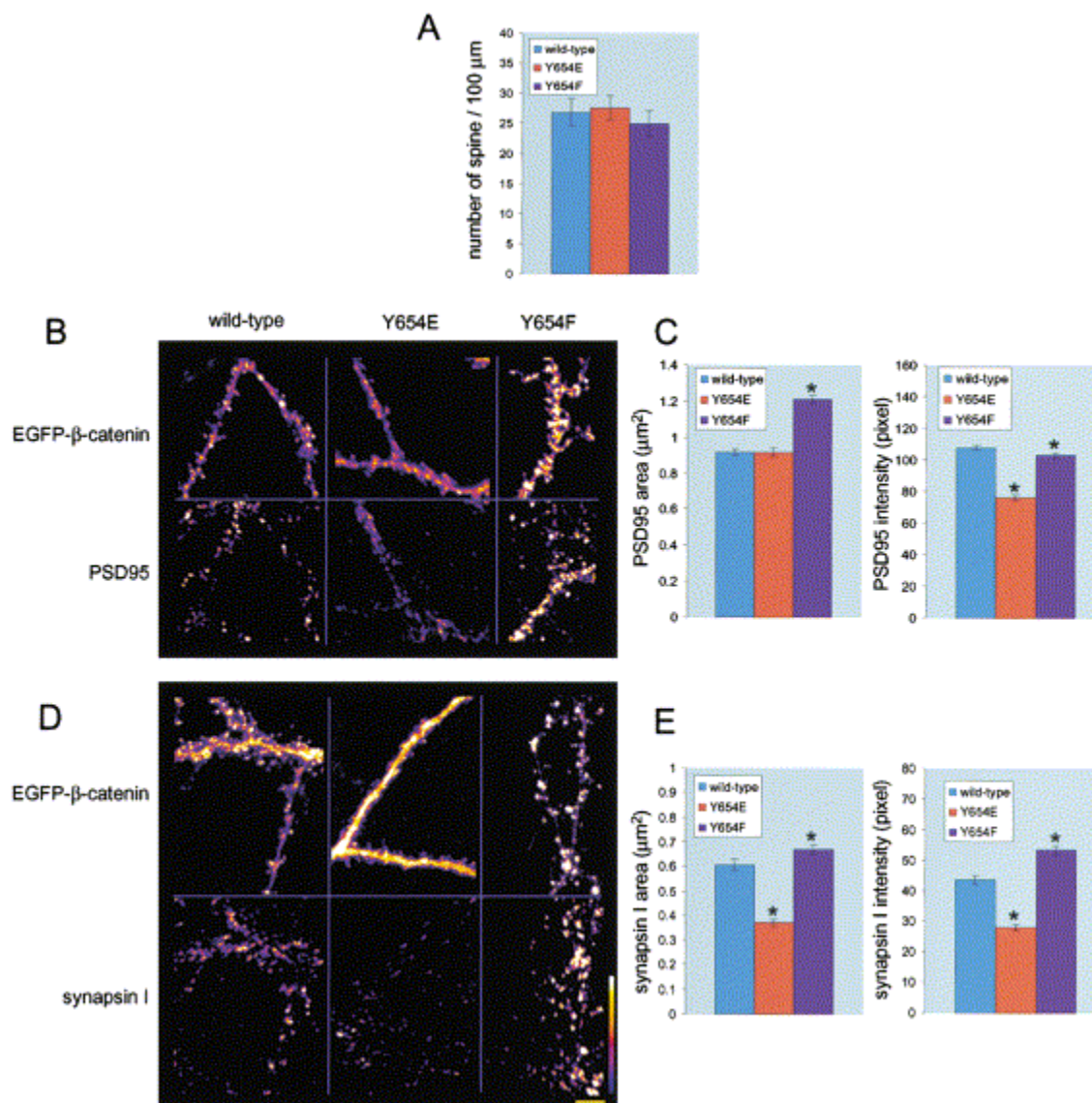


Figure 2. Mutation of a β -catenin tyrosine residue affects the size and intensity of presynaptic and postsynaptic protein clusters.

A. The mean number of spines did not differ between the groups, with N = 22, N = 22, and N = 22, respectively. B. EGFP- β -catenin with anti-PSD95 immunostaining. C. Summary data (n = 12 for each group). D. EGFP- β -catenin and anti-synapsin I immunostaining. E. Summary data (n = 10 for each group). Scale bars: 20 μm (Murasu, Mosser et al. 2002).

Because cadherins span the synapse through their *trans* interactions, we reasoned that a postsynaptically driven increase in the interaction of β -catenin with cadherin might also cause changes across the synapse in presynaptic structures. Two other studies have observed increases in immunolabeling for presynaptic proteins following synaptic plasticity (Antonova, Arancio et al. 2001 and Bozdagi, Shan et al. 2000). We thus conducted a similar analysis of a presynaptic protein, synapsin-I, to determine whether the size or intensity of synapsin-I-positive puncta were altered by the expression of either β -catenin mutant. Dr. Murase immunostained transfected cells for synapsin-I and as above, I analyzed only the synapsin-I-positive puncta that were associated with spines from a β -catenin-EGFP-expressing neuron.

Both the size and intensity of synapsin-I puncta from Y654F mutants were significantly enhanced, relative to wild-type or Y654E-expressing cells (figure 2, D and E). In contrast, the synapsin-I clusters in Y654E-expressing neurons were significantly smaller and less intense than those observed in wild-type or Y654F-expressing cells. These data show that increases in spine β -catenin are associated with increases in the size and intensity of synapsin-I clusters, whereas decreases in spine β -catenin are associated with smaller and less intense synapsin-I clusters.

These data suggest that the local concentration of β -catenin in spines can drive changes in presynaptic protein clustering across the synaptic junction, which may reflect the transsynaptic action of cadherins (summarized in figure 3).

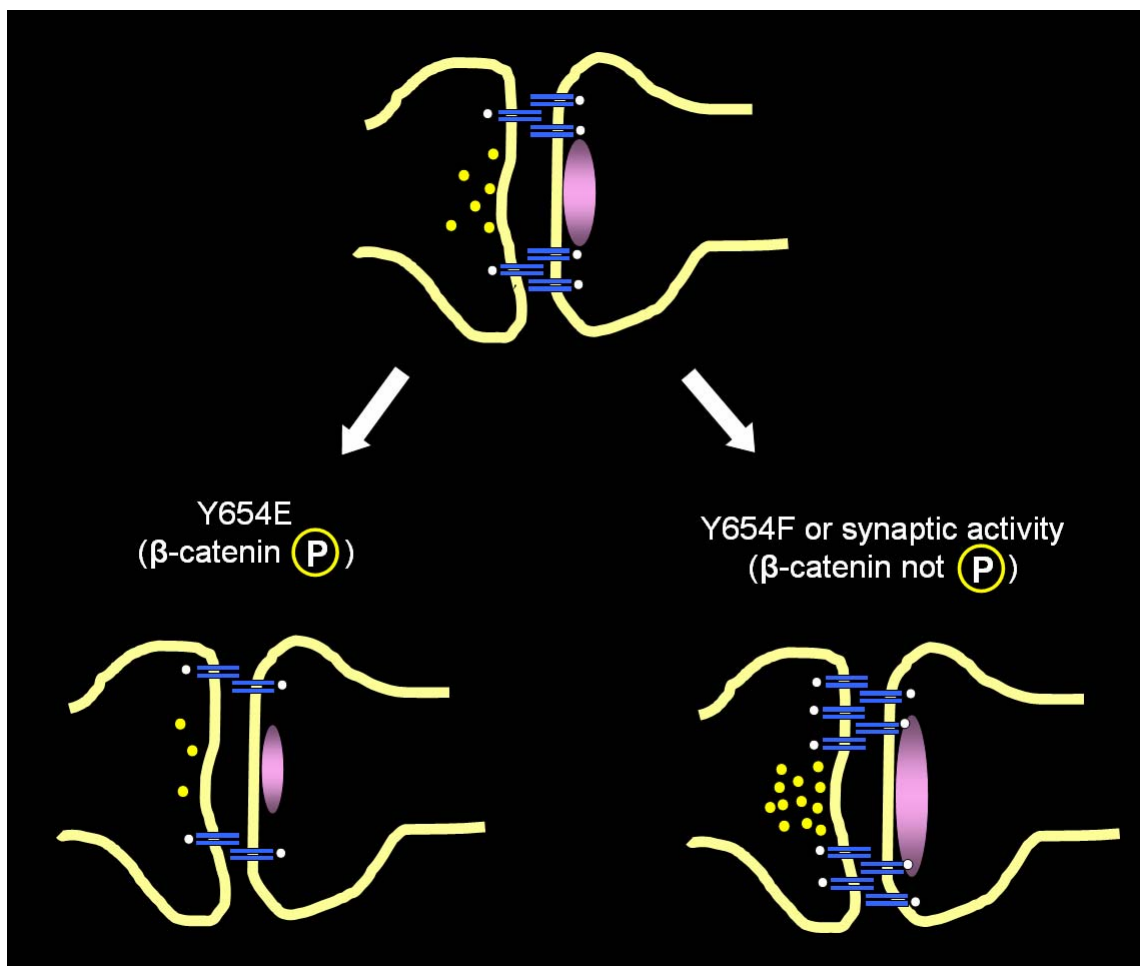


Figure 3. Scheme of β -catenin's redistribution following synaptic activity or mutation of tyrosine 654.

The symbols in the diagram represent the following: cadherin dimers, blue bars; β -catenin, white circles; the PSD, pink oval; synaptic vesicles, yellow spheres. Conditions that lead to the phosphorylation of β -catenin or mimic the phosphorylation (the Y654E mutant) may result in decreased β -catenin cadherin interactions, decreased adhesion, and decreases in the PSD and the synaptic vesicle pool size of associated presynaptic terminals. Conversely, synaptic activity or conditions that favor a dephosphorylated state for β -catenin lead to increased association with cadherins, increases in the PSD, and increases in the synaptic vesicle pool size of associated presynaptic terminals (adapted from Murase, Mosser et al. 2002).

Chapter IV

DEVELOPMENT OF CADHERIN FRET REPORTERS

In order to better understand the homophilic interactions of cadherins in living cells, I undertook the construction of a series of pairs of cadherin fluorescent fusion proteins to use in FRET experiments. The goal of the experiments was to detect changes in cadherin conformational and binding states by monitoring energy transfer at the cell membrane junction between adjacent cells expressing cadherins labeled with FRET donor and acceptor fluorophores, respectively.

Epitope tagging approaches

My initial efforts involved creating small-epitope-tagged cadherins with the plan of using fluorescent primary antibodies to label the epitope tags with FRET donor and acceptor fluorophores. I inserted HA and FLAG epitopes at several points in the E-cadherin extracellular region. These insertion points were chosen with the following considerations in mind: to optimize the relative distance of each molecule in an intact cellular junction for energy transfer, to use sites accessible to an exogenously introduced antibody, and to avoid regions involved in Ca^{2+} binding, cadherin dimerization, or cadherin structure (based on structural data obtained from Shapiro, Fannon et al. 1995 and Overduin, Harvey et al. 1995) (figure 4).

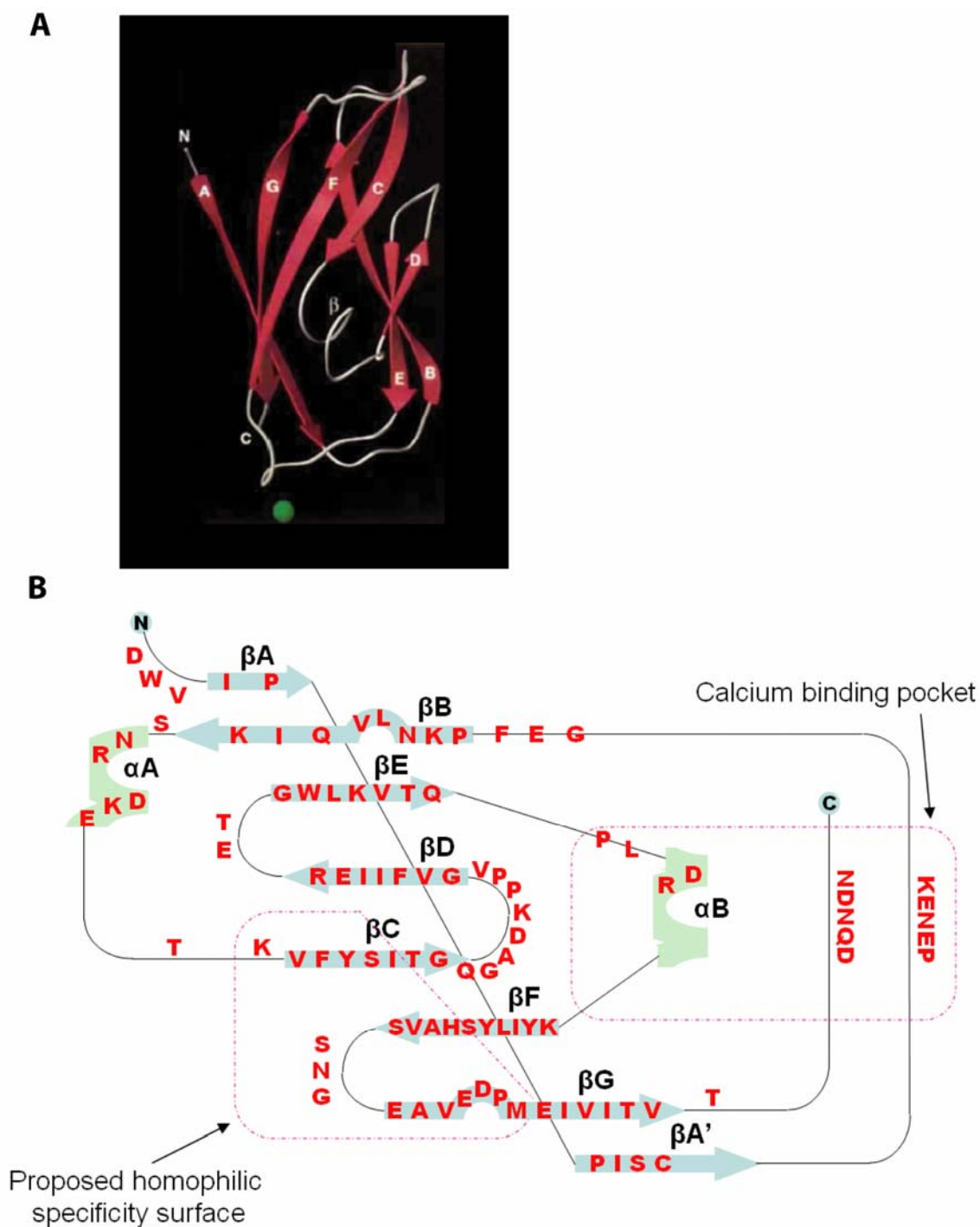


Figure 4. Structure of the N-terminal EC domain (EC1) of E-cadherin.

A. Ribbon diagram of EC1. Each β -strand is labeled and the Ca^{2+} binding site is indicated by the green sphere. B. Schematic drawing of the domain topology with the 7 β -strands (βA through βG) displayed in light blue and the two α -helices in light green. Residues involved in the proposed homophilic specificity surface and the Ca^{2+} binding

site are indicated by the purple dashed lines (adapted from Overduin, Harvey et al. 1995 and Shapiro, Fannon et al. 1995).

This approach served mostly to demonstrate the cadherin sensitivity to any molecular “mucking around,” particularly when molecules were inserted near the N-terminus. Some previous work in the laboratory had generated E-cadherin N-terminally tagged with EGFP; the fusion protein could be expressed in cultured cells, and the GFP moiety was fluorescent, but the molecule was not trafficked correctly, and got stuck in the Golgi and endoplasmic reticulum (ER). Similar to this, my first generation of small-epitope tagged cadherins (with the tags inserted between EC1 and EC2) were also sequestered in the Golgi and ER and were only internally expressed, rendering them useless as FRET reporters.

For the next round of fusions I decided to insert the tags more C-terminally in the extracellular domain; on a loop in EC4 and between EC4 and EC5. These constructs were properly trafficked and inserted into the membrane, but I was not able to successfully immunolabel live cells expressing them, possibly due to the relative inaccessibility of the epitope tags in the cell junction.

Fluorescent protein approaches

Based on the lack of success described above, I decided to create fluorescent fusion protein (ECFP and EYFP) insertions instead. Unfortunately, this proved equally difficult: inserting ECFP or EYFP into the same point between EC1 and EC2 used for the small-epitope tags caused the same problems with membrane expression as seen with the epitope fusions. Inserting CFP/YFP into a loop in EC3 finally yielded a cadherin-EGFP-variant fusion that was properly expressed on the membrane, and could be

immunolabelled in live cells with either anti-cadherin antibodies or anti-GFP antibodies. However, the GFP-variant was not fluorescent, suggesting that its position in the cadherin structure resulted in misfolding.

Transposon-mediated functional insertion of fluorescent proteins in N-cadherin

Dr. Chin-Yin Tai, a postdoctoral scholar in our laboratory, used a transposon-mediated random insertion strategy to successfully create a GFP-N-cadherin intramolecular fusion that was both membrane expressed and properly folded and fluorescent. The bacterial transposon, Tn5, known for its well-known properties of high efficiency ($>10^6$) and randomness, was used. This enzyme recognizes a 19-base-pair inverted repeat of the transposon-containing DNA (linear or circular) and makes a 9-base-pair staggered nick in the target DNA. After transposition, this nick is repaired and subsequently generates a 9 base pair duplication of the target sequence immediately flanking the transposon (figure 5A). To identify clones that possess the correctly inserted GFP, colony polymerase chain reaction (PCR) was chosen since this method allowed the screening of hundreds of colonies without DNA amplification and purification (figure 5B). Three 5'-end primers covering the whole N-cadherin coding region and one 3'-end primer within GFP were designed (see materials and methods for details). To reduce the number of reactions that were required, several (~5) colonies were pooled into 1 reaction. This allowed a rapid elimination of those colonies that fail to produce a positive result. Colonies that express the in-frame fusion protein were selected by transiently transfecting all clones into HEK293 cells, to directly visualize GFP fluorescence (figure 5C). Lastly, the full-length N-cadherin with intramolecular GFP insertions was restored. During the transposition, a stop codon was inserted between GFP and the kanamycin-resistant gene,

which created a truncated N-cadherin GFP fusion. A restriction enzyme (SmaI) digestion followed by self-ligation and bacterial transformation restored the full length N-cadherin GFP fusion (figure 5D). Upon completion of the screen, all remaining clones were ready for functional assays.

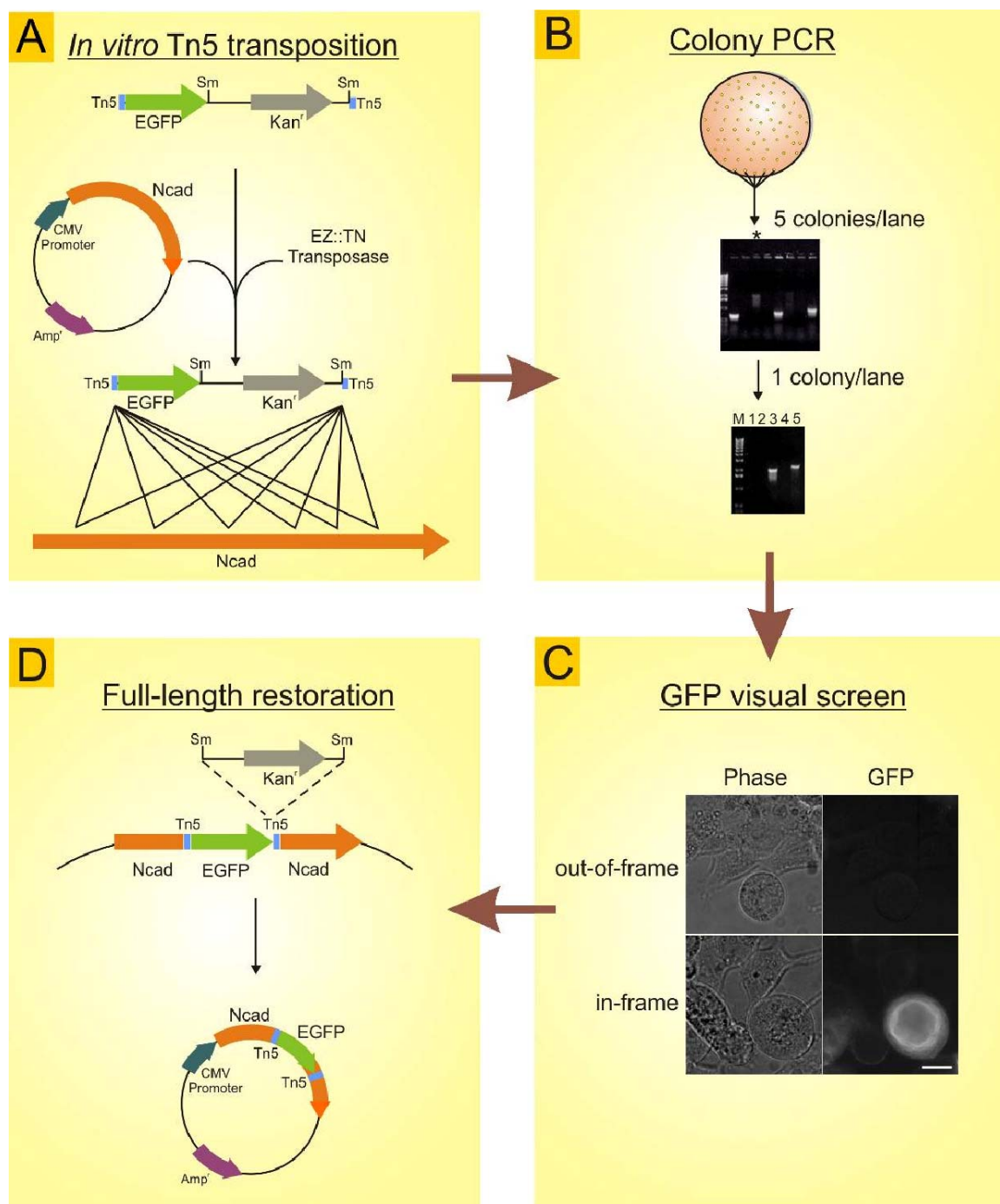


Figure 5. Overview of the bacterial transposon-mediated random insertion.

A. The target plasmid DNA (pCXN2-NCad) was incubated with the linearized transposon-containing plasmid DNA (pBNJ24.6), and EZ:TN transposase (Epicentre) at 37°C for 2 hours. The transposed products were selected by the double antibiotic resistance of ampicillin (selection marker for the target plasmid) and kanamycin (Kan^r , selection marker located downstream of EGFP). B. Correctly oriented GFP insertional clones were identified by two rounds of colony PCR reactions. C. HEK293 cells were

transfected with DNA of the selected clones and GFP signals were visualized under the fluorescent microscope. D. All fluorescent clones were digested with restriction enzyme, SmaI, and re-ligated *in vitro*. Recovered full-length clones were isolated after transforming into bacterial host strain. Scale bar: 5 μ m (From Dr. Chin-Yin Tai).

In order to function in FRET assays, the clones need to be expressed at cell junctions. A preliminary screen was performed as described above for 509 colonies and 23 candidate clones were obtained. All 23 clones were transfected into HEK293 cells after the full-length restoration procedure. When the fluorescence was visualized in intact transfected cells, 10 clones exhibited localization at the adherens junctions, the expected location for a functional cadherin protein. These clones were then subjected to DNA sequencing to identify the exact site of insertion - 6 out of 10 clones had GFP inserted in the extracellular domain of N-cadherin (figure 6A). In this first screen, 2 preferential insertion sites were noted: one is located between the fifth EC and the transmembrane domain, and the other is in the middle of the cytoplasmic domain. In addition, no insertion sites within the third to the fifth EC domain were found, suggesting that the Tn5-mediated transposition is not absolutely random. However, 4 clones that had GFP inserted in the distal extracellular region were found (figure 6B). Among them, clone TS25 had the brightest adherens junction signal in HEK293 cells. As such, this clone was chosen for the initial FRET experiments. After clones that express well at junctions were identified, I cloned ECFP and EYFP in the place of GFP, and the resulting constructs were transfected into L cells for an aggregation assay. Note that L cells lack endogenous cadherins but contains all catenins and have been used extensively for cadherin-dependent adhesion functional assays (Nagafuchi, Shirayoshi et al. 1987). When successfully transfected with cadherins, L cells exhibit adhesion and aggregation

that is dependent on extracellular Ca^{2+} (Nagafuchi, Shirayoshi et al. 1987). As L cells are notoriously hard to transfect and measures of aggregation require high transfection efficiency, stable lines that express either the Cad-CFP (FRET donor) or Cad-YFP (FRET acceptor) were constructed. After one month of continuous selection and expansion from a single colony, 10 independent clones were picked for each construct. Western blotting analyses revealed 3 lines that stably express Cad-CFP and 6 lines that stably express Cad-YFP. A calcium-dependent aggregation assay was performed for all clones; representative results are shown in figure 3C. In addition, it was found that each fusion protein interacts with β -catenin via immunoprecipitation assays (figure 6D).

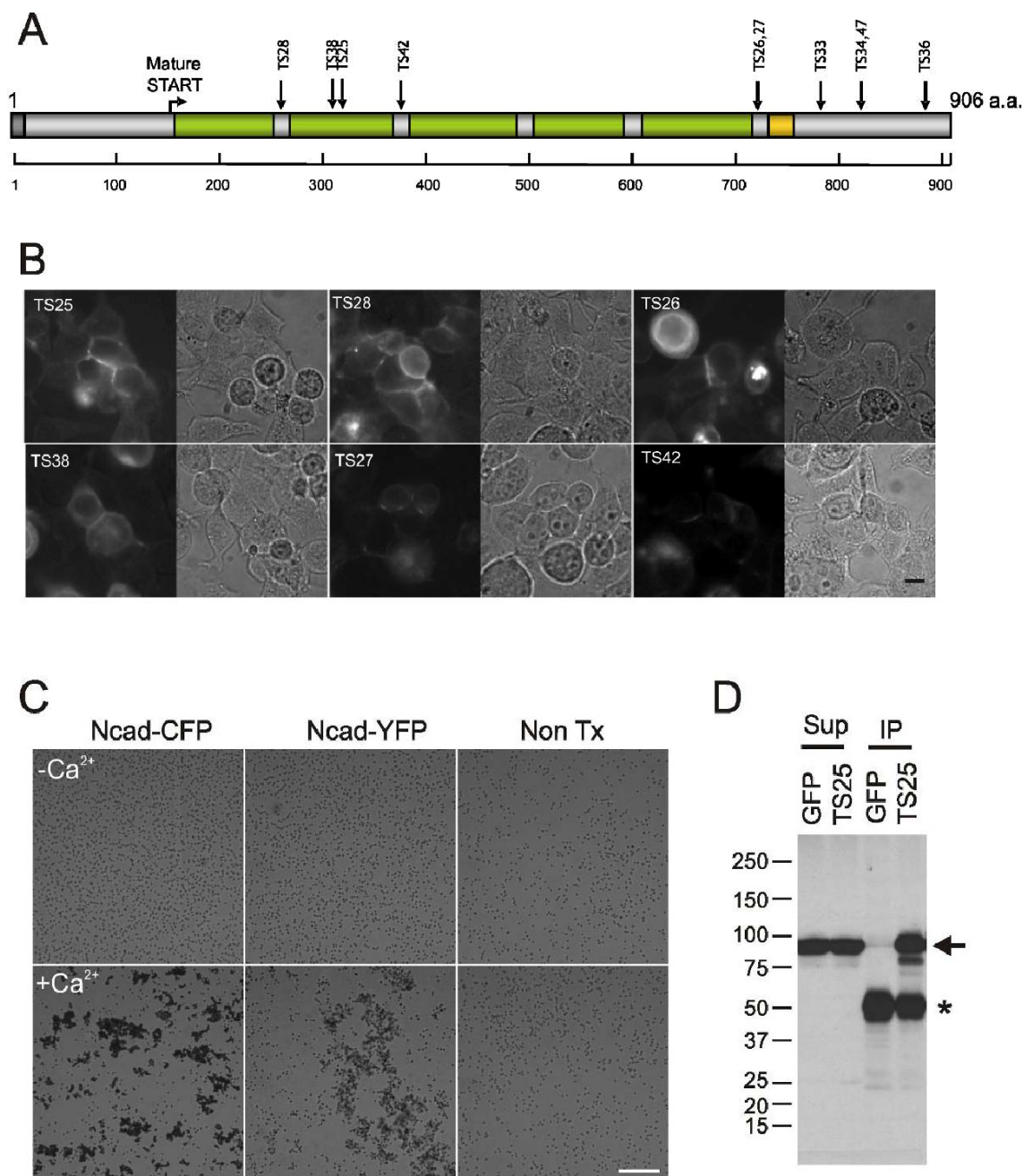


Figure 6. Functional assays of GFP-N-cadherin fusion proteins.

A. Schematic summary diagram of GFP insertion sites. The linear N-cadherin protein structure is colorized according to the following: dark grey represents the signal peptide; green represents the extracellular domains; yellow represents the transmembrane domain. The segment beyond the transmembrane domain contains the cytoplasmic domain, which binds members in the catenin family. B. Adherens junction localization of 6 GFP-N-cadherin clones that have GFP inserted at the extracellular domain. C. Calcium-dependent homophilic interactions of the CFP or YFP fusion derived from the TS25 clone in L cells. Non Tx represents nontransfected cells. D. β -catenin interacts with the

GFP-N-cadherin fusion protein (arrow: 90 kDa β -catenin, *: IgG heavy chain). Scale bars: in B: 5 μ m; in C: 50 μ m (From Dr. Chin-Yin Tai).

Monitoring cadherin interactions via acceptor bleaching (adFRET)

Acceptor bleaching or depletion is a simple and rapid method of measuring FRET that avoids some of the complications in other FRET measurement techniques, as it provides “*in situ*” (at every pixel of interest) generation of the reference state of the nonFRETing donor fluorophore. Simply put, the bleaching of the acceptor increases the donor fluorescence observed owing to dequenching of the signal (figure 7).

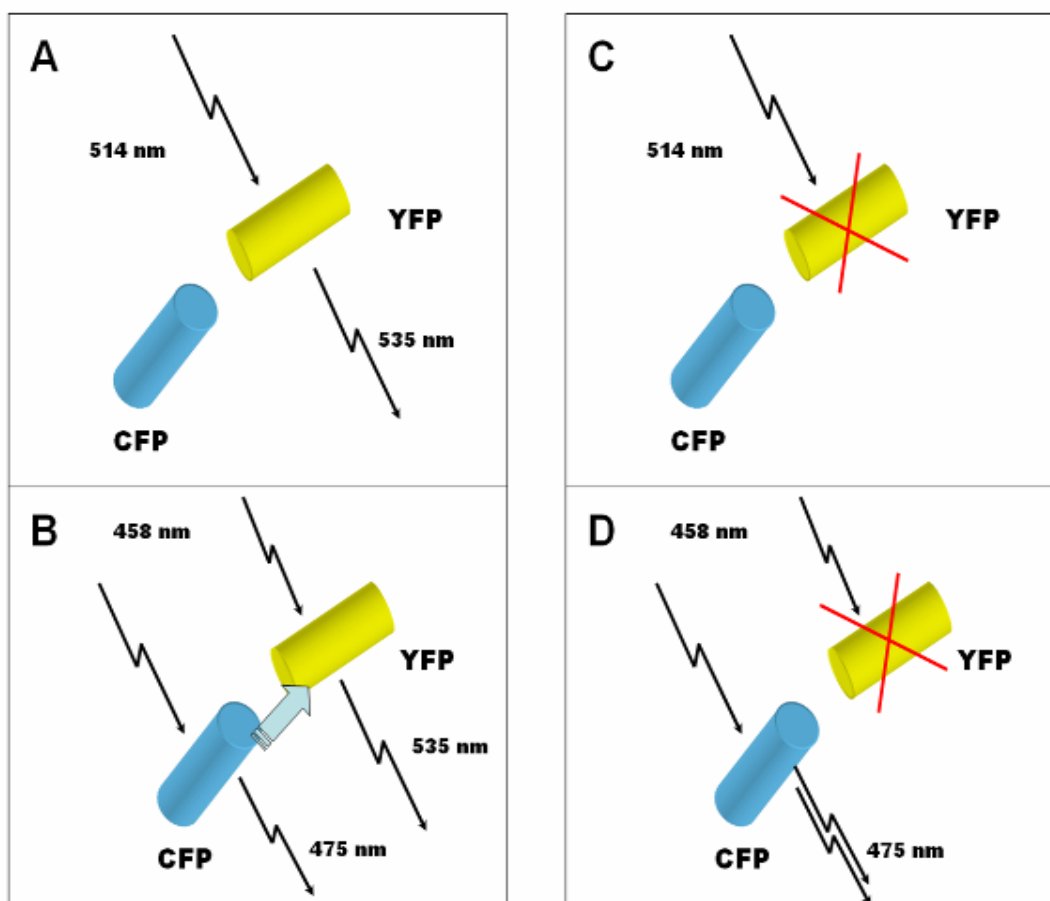


Figure 7. Overview of FRET and the acceptor bleach FRET experiment.

A. Cells expressing both donor and acceptor are illuminated with 514 nm laser light, exciting YFP (the FRET acceptor) and resulting in acceptor emission. B. The same cell is illuminated with 458 nm laser light, exciting primarily CFP, but also minimally exciting YFP. If donor and acceptor are in close enough proximity and oriented properly, FRET will occur, leading to increased acceptor emission. C. If the acceptor is depleted (through irreversible photobleaching), illumination with 514 nm light yields decreased acceptor emission (in practice, bleaching is rarely complete, leaving some intact acceptor molecules to fluoresce). D. When the acceptor is photobleached, FRET is no longer possible, so when the acceptor-depleted cell is illuminated with 458 nm light, the donor fluorescence is increased relative to B.

To determine whether the N-cadherin fusion proteins can detect cadherin-cadherin *cis* interactions, I doubly-transfected HEK-293 cells with ECFP- and EYFP-tagged N-cadherin (generated from GFP-Ncad clone TS25). I then imaged the cells using an LSM Meta laser scanning confocal microscope and unmixed the CFP and YFP spectra as described in the methods section (figure 8). Upon acceptor bleaching, modest yet detectable donor dequenching was observed, indicating detectable FRET between cadherins, presumably involved in *cis* interactions. Longer bleaching times and more thorough bleaching led to increased donor dequenching, as expected if the acceptor bleach and donor dequench are rooted in the same process (figure 8F).

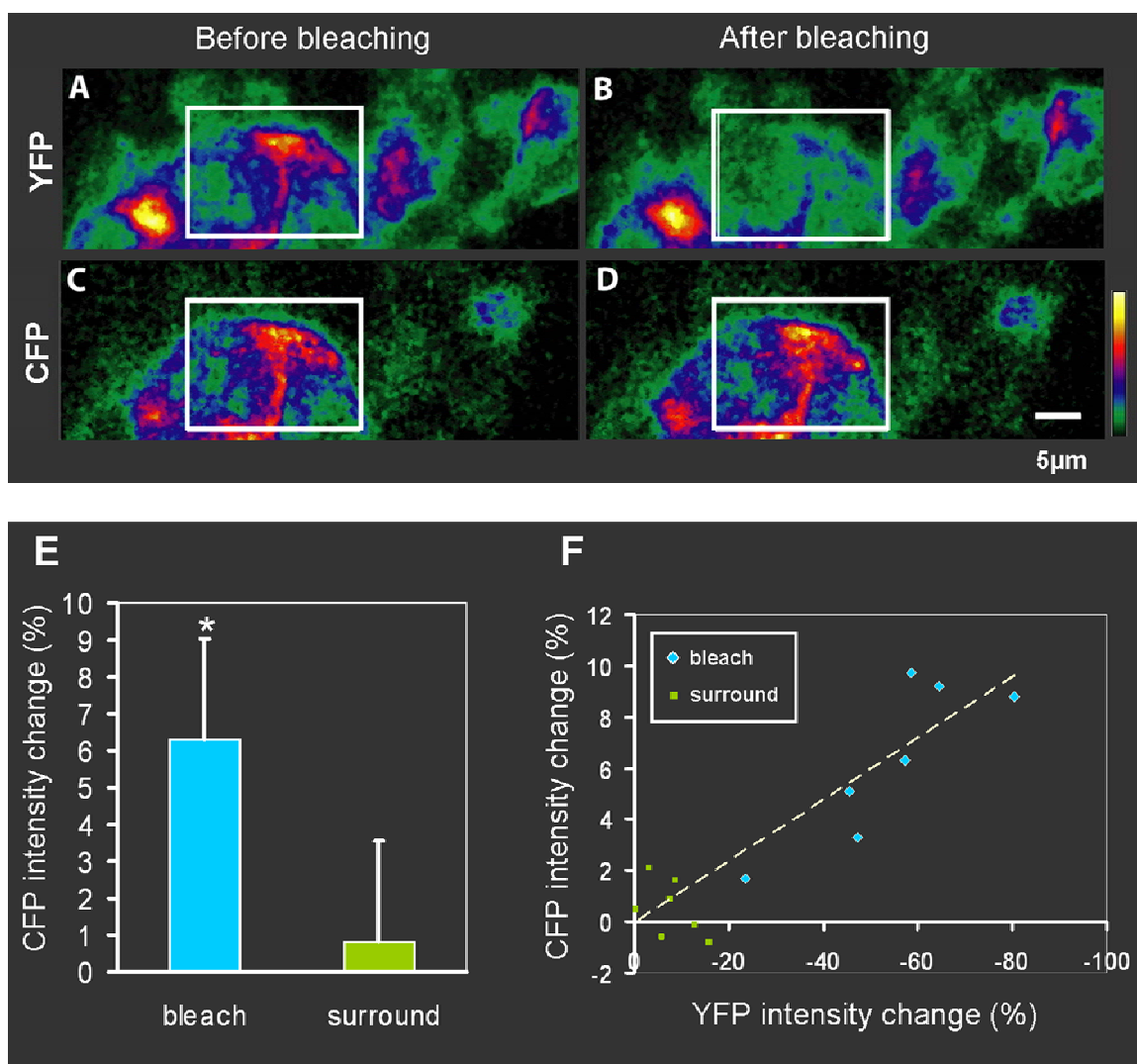


Figure 8. adFRET in HEK-293 cells expressing both CFP-N-cadherin and YFP-N-cadherin revealing cadherin *cis* interactions.

A. LSM Meta laser scanning confocal microscope generated YFP signal (linear unmixing of separately obtained YFP and CFP spectra was used to generate YFP-only signal). B. Post-acceptor-bleach YFP signal. C. LSM Meta laser scanning confocal microscope generated CFP signal. D. Post-acceptor-bleach CFP signal (white boxes represent the bleached area). E. Fluorescent intensities of bleached ROI and surrounding nonbleached areas were quantitated and the percent change of the donor signal was calculated. F. More thorough bleaching leads to increased donor dequenching, as expected if the YFP bleaching and the CFP dequenching are connected through and originating from the same process. Scale bar: 5 μ m.

To investigate whether *trans* interactions (across cellular junctions) between labeled cadherins expressed in different cells could be detected by adFRET, I first replaced the ECFP and EYFP tags with Cerulean and Venus, respectively, to provide increased donor and acceptor brightness and improved signal-to-noise ratio (Rizzo, Springer et al. 2004; Nagai, 2002). I then transiently transfected COS-7 cells with Cerulean- *or* Venus-tagged N-cadherin (generated from GFP-Ncad clone TS25), and trypsinized and mixed the separately transfected cultures, before replating the cells in glass-bottomed dishes for imaging and analysis (figure 9). Upon acceptor bleaching, donor dequenching was comparable to that observed in the doubly transfected cells. A similar linear relationship was observed between the magnitude of acceptor bleaching and donor dequenching (figure 9G).

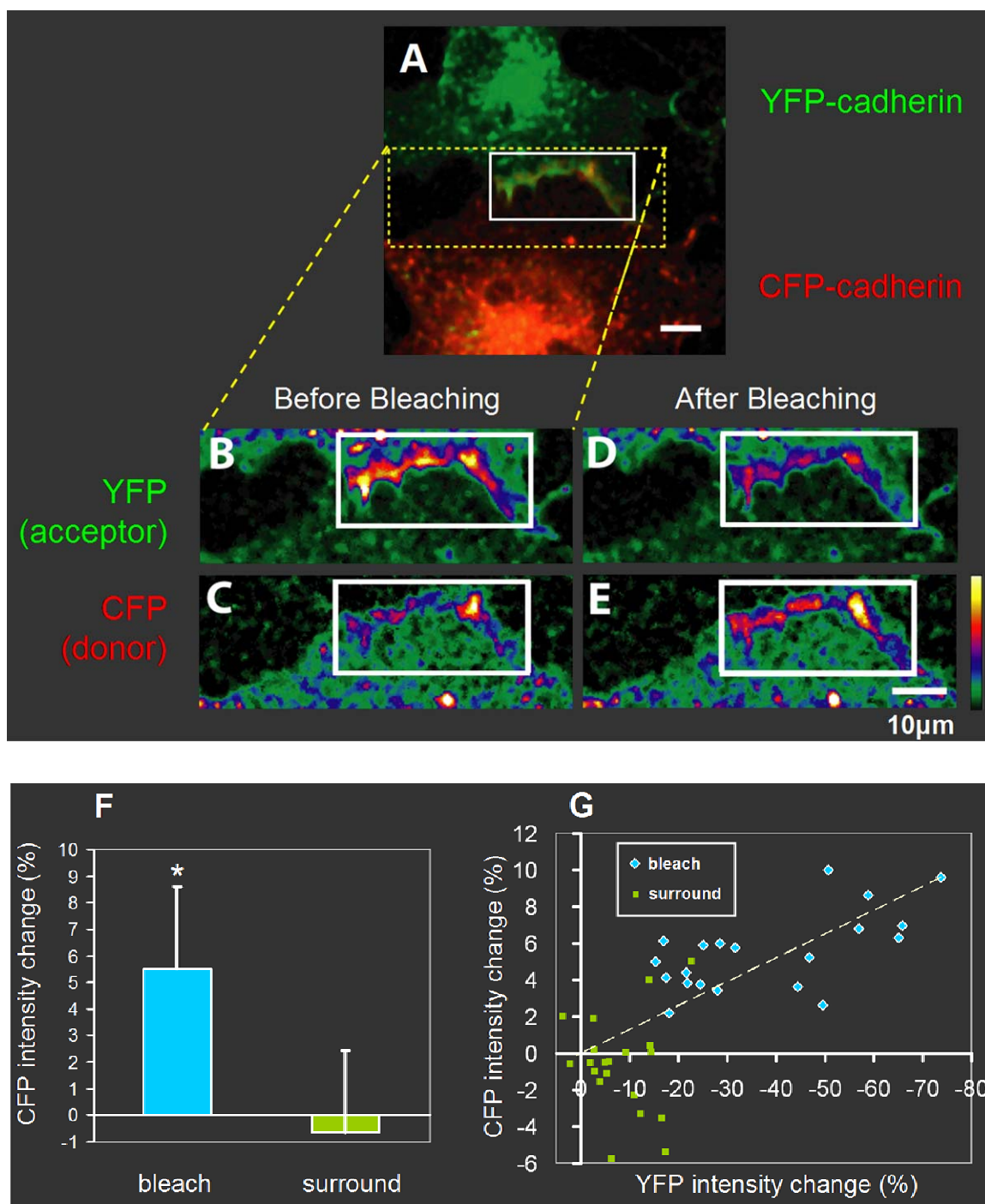


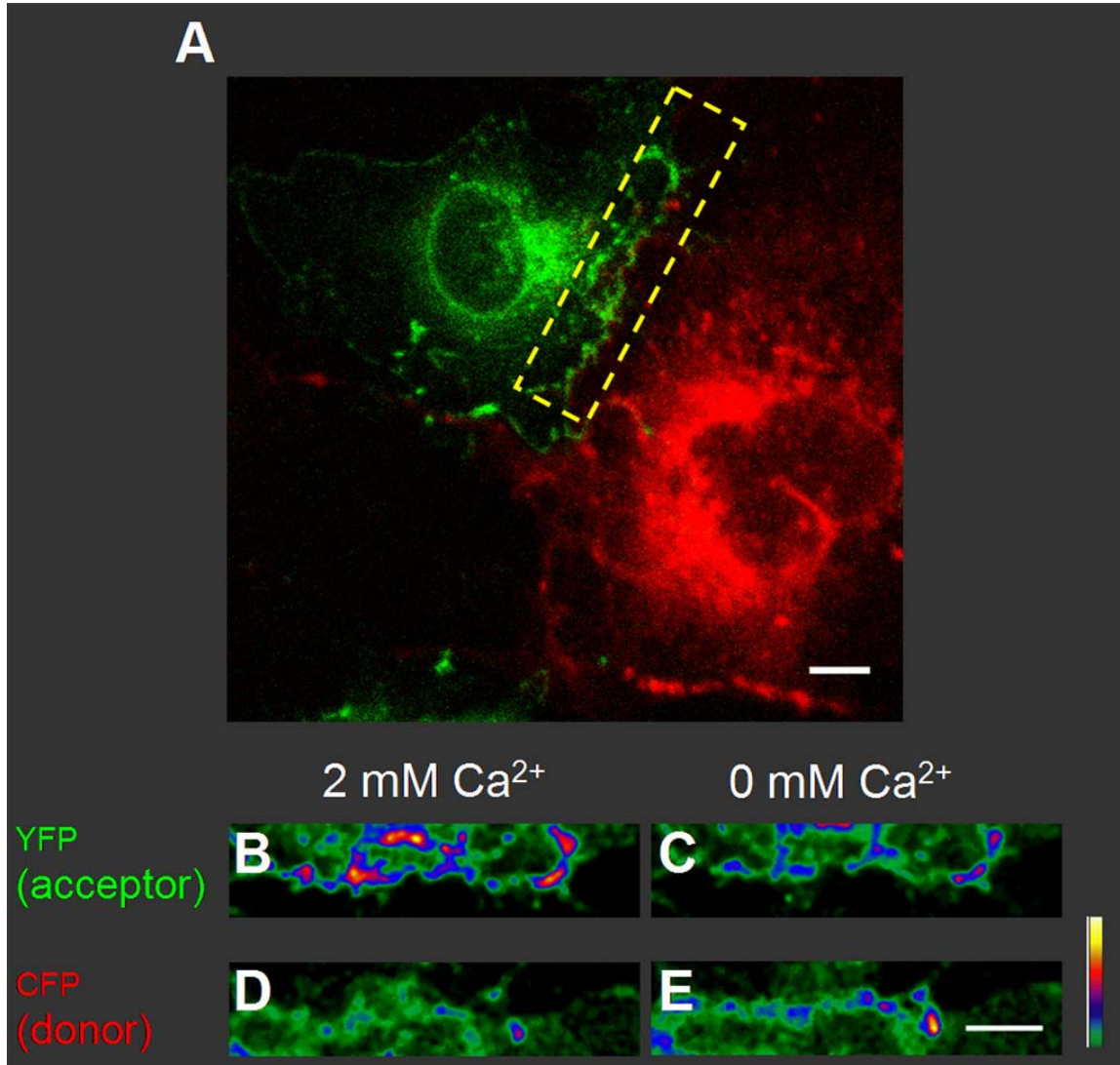
Figure 9. adFRET at cell junctions between COS7 cells separately expressing Cerulean-N-cadherin or Venus-N-cadherin.

COS7 cells were transfected with each construct (Venus- and Cerulean-Ncad) separately. After 8 hours, cells were trypsinized and replated together for another 24 to 30 hours. **A**. An example of the co-culture. Cells expressing Venus-Ncad are shown in green and cells expressing Cerulean-Ncad are shown in red. If two neighboring cells were found to express different fluorescent proteins and a clear junction was visible, then adFRET was

assayed at the junction/region of Venus/Cerulean overlap (dashed yellow outline shows region shown in B-E; solid white outline shows bleached area). B. LSM Meta laser scanning confocal microscope generated Venus signal (linear unmixing of separately obtained Venus and Cerulean spectra was used to generate Venus-only signal). C. LSM Meta laser scanning confocal microscope generated Cerulean signal. D. Post-acceptor-bleach Venus signal (white box represents bleached area). E. Post-acceptor-bleach Cerulean signal. F. Fluorescent intensities of bleached ROI (white box) and surrounding nonbleached areas were quantitated and the percent change of donor signal was calculated. G. More thorough bleaching leads to increased donor dequenching, as expected if the YFP bleaching and the CFP dequenching are connected through and originating from the same process. Scale bar: 10 μm .

Visualizing changes in cadherin-cadherin interactions induced by changes in extracellular Ca^{2+} concentration

As the Cerulean- and Venus-N-cadherin constructs exhibited detectable changes in FRET upon acceptor bleaching, I concluded that the FRET donor and acceptor pair must be in close proximity and in the correct orientation in the intact cell junction. I next manipulated the extracellular Ca^{2+} concentration. A decrease in the extracellular Ca^{2+} concentration should cause a cadherin conformational change and unbinding of the homophilic pairs. In the simplest experiment, FRET was monitored before and after extracellular Ca^{2+} was decreased by perfusion with new reduced Ca^{2+} media. We determined that the addition of calcium chelators was the most efficient means to rapidly quench Ca^{2+} . Co-cultured, singly-transfected COS-7 cells were first imaged in HBS containing 2mM Ca^{2+} , which was then washed off and replaced with HBS lacking Ca^{2+} and containing 2mM EGTA, to chelate any remaining Ca^{2+} . The cells were then imaged again and FRET donor and acceptor signals were compared to the baseline, Ca^{2+} image. We observed that reducing Ca^{2+} in the extracellular solution led to a significant loss of FRET signal at COS-7 cell junctions expressing FRET pairs (figure 10).



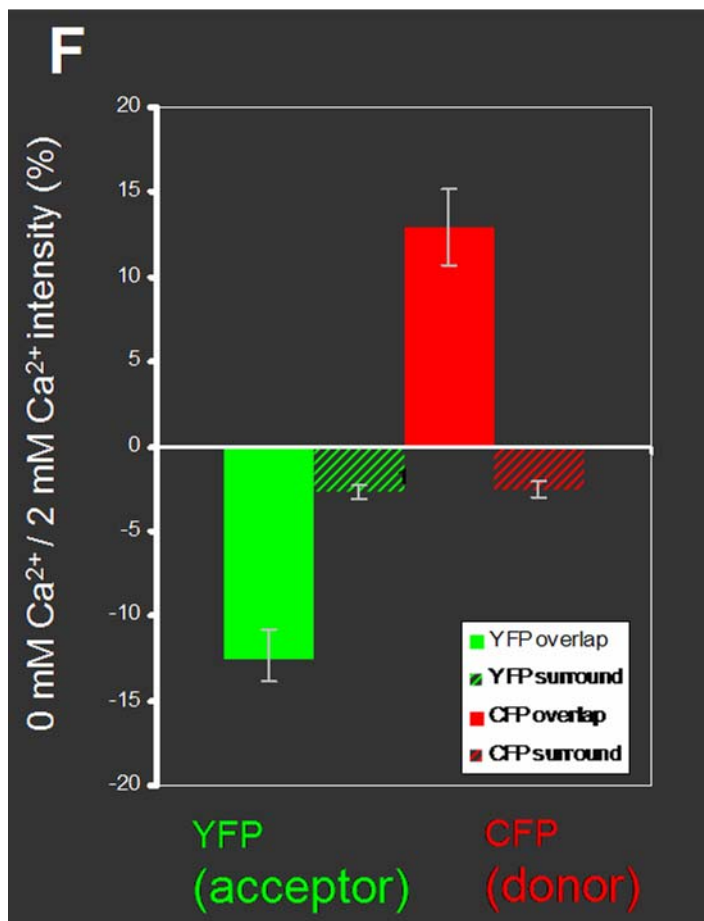


Figure 10. Monitoring changes in FRET induced by changes in extracellular Ca²⁺ concentration in COS7 cells.

COS7 cells were transfected with each construct (Venus- and Cerulean-Ncad) separately. After 8 hours, cells were trypsinized and replated together for another 24 to 30 hours. A. Representative image of a pair of cells; cells expressing Venus-Ncad are shown in green and cells expressing Cerulean-Ncad are shown in red (dashed yellow outline shows region shown in B-E). B. LSM Meta laser scanning confocal microscope generated Venus signal (linear unmixing of separately obtained Venus and Cerulean spectra was used to generate Venus-only signal). C. Venus signal after removal of extracellular Ca²⁺. D. LSM Meta laser scanning confocal microscope generated Cerulean signal. E. Cerulean signal after removal of extracellular Ca²⁺. F. Fluorescent intensities of area of Venus /Cerulean overlap and surrounding nonoverlapping areas were quantitated and the percent change of donor (Cerulean: red bars) and acceptor (Venus: green bars) signals was calculated. Scale bars: 10 μ m.

Having observed that reducing Ca^{2+} in the extracellular solution leads to a significant loss of FRET signal at COS-7 cell junctions expressing FRET pairs, I next used repeated, fast scans of the junction between transfected cell pairs to monitor FRET changes due to changes in extracellular Ca^{2+} during perfusion, allowing me to examine the dynamics of cadherin-cadherin interactions on a shorter time scale.

Baseline images of COS-7 co-cultures were taken during perfusion with media containing 2mM Ca^{2+} ; after a baseline period of 5 scans, the perfusate was switched to media containing 0mM Ca^{2+} and EGTA; at the same time, additional EGTA was added to the dish. This caused a rapid loss of FRET, as indicated by the increase in Cerulean signal and concomitant decrease in Venus signal in areas with Cerulean/Venus overlap (figure 11). After further scanning, imaging was stopped (to allow for complete replacement of the residual HBS in perfusion tubing), and the perfusate was switched back to media containing Ca^{2+} (2mM). This can be observed as the discontinuity between scans 30 and 31 and reflects a period of ~1 minute. After perfusate in the pump had been exchanged, imaging was reconvened and a return of FRET was observed, reflecting the reassociation of cadherins in the presence of Ca^{2+} .

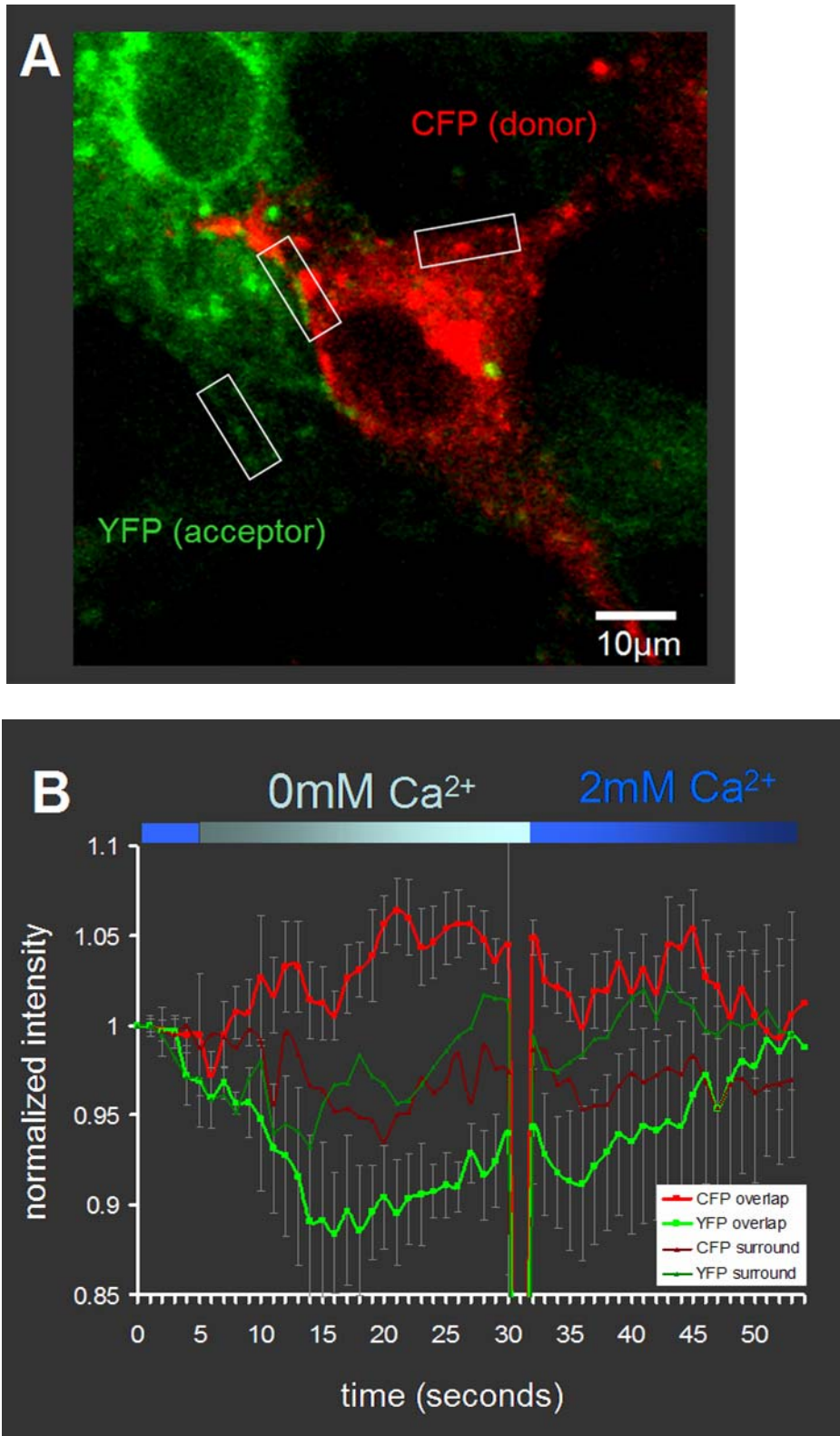


Figure 11. Monitoring changes in FRET induced by changes in extracellular Ca²⁺ concentration in COS7 cells.

COS7 cells were transfected with each construct (Venus- and Cerulean-Ncad) separately. After 8 hours, cells were trypsinized and replated together for another 24 to 30 hours. A. Representative image of the pair of cells imaged to generate the intensity profile in (B). Cells expressing Venus-Ncad are shown in green and cells expressing Cerulean-Ncad are shown in red. B. Cerulean and Venus signals were monitored over time as extracellular Ca^{2+} concentration was manipulated. Cell media was switched from 2 mM Ca^{2+} to 0 mM after scan #5, then back to 2 mM Ca^{2+} after scan #30, as described in the text. Bold traces are Cerulean (red trace) and Venus (green trace) signals measured at the cell junction where Cerulean/Venus overlap occurs (box 1 in A); dimmer traces (control) are measured in areas with no Cerulean/Venus overlap (boxes 2 and 3 in A). Colored bars above plot represent Ca^{2+} concentration used in perfusion; black bars = 2 mM Ca^{2+} , red bar = 0 mM Ca^{2+} + 2mM EGTA. Gap between red and black bar represents period of perfusate replacement in tubing. Scale bar: 10 μm .

These data show that the TS-25 based XFP-cadherin clones exhibit FRET when expressed in living cell junctions, and can be used to monitor and detect changes in cadherin conformational and adhesive state in response to changes in extracellular Ca^{2+} concentration. I believe they will be valuable tools in the effort to determine the cadherin response to synaptic activity and to elucidate a cadherin role in synaptic plasticity.

Chapter V

DISCUSSION AND FUTURE DIRECTIONS

Members of the cadherin family of cell surface glycoproteins have long been known to be involved in many aspects of cell-cell adhesion and recognition. In recent years, numerous studies have suggested a role for cadherins in the regulation of synaptic plasticity, both morphological (structural) and functional. The work described here contributed to expanding knowledge of cadherin function, and eventually the role thereof in synaptic modulation through the development of reporters of cadherin adhesive state. These reporters should prove valuable tools in the study of cadherins and their roles, both in the nervous system and elsewhere.

Construction of cadherin FRET reporters

In chapter IV of my thesis work, I have described the development of fluorescent cadherin molecules for use in FRET experiments. As described, there were many difficulties in generating cadherins that were both properly membrane expressed and fluorescent. A particular impediment to this was the apparent sensitivity of cadherin to intramolecular insertions, especially near its N-terminus. This sensitivity may be due, in part, to the proteolytic cleavage known to be required for production of mature cadherin from its preformed, inactive precursor (Ozawa and Kemler 1990; Wheeler, Parker et al. 1991). As is known to be the case for other proteins matured in the constitutive secretory pathway as cadherin is, precursors are synthesized in the endoplasmic reticulum, and are then trafficked through the *cis* and *trans* Golgi (Pasdar, Krzeminski et al. 1991). Pro-protein cleavage then needs to occur before cadherins can be trafficked to the cell membrane. It is currently not known which factors control and trigger the initiation of cadherin processing. However, Posthaus et al. have provided some evidence concerning

the enzyme(s) mediating E-cadherin and the desmosomal cadherins maturation (Posthaus, Dubois et al. 1998, 2003). Using a baculovirus co-expression system it was demonstrated that furin, a member of the subtilisin-like convertase family, is a proE-cadherin processing enzyme (although they were not able to determine with certainty that furin was the sole enzyme responsible).

Initial insertions in the first two EC repeats (EC1 and EC2), whether small epitope tag, or XFP fusions, yielded cadherins that were misprocessed and sequestered in ER and Golgi. The insertion points chosen were not near the regions known to be important for the pro-processing of cadherin, but may still have interfered with the action of the molecules necessary for cleavage or trafficking

The one site arrived at by making “intelligent guesses” that I was able to successfully membrane express an XFP-cadherin fusion at was on a loop in EC3, between β -strands C and D. These fusion proteins were properly expressed in the membrane, yet not fluorescent, as discussed in chapter IV. Interestingly, the site where GFP was inserted by random transposon insertion in clone TS25 was 4 amino acids away from the site I had chosen based on the published EC structures. This distance of 4 residues apparently made all the difference, as TS25 is properly expressed in the membrane and fluorescent, while my initial EC3-XFP fusions did not fluoresce. I think this demonstrates the power of a “shotgunned” and selectable approach, such as the transposon insertion technique.

Geometry of cadherins in cell junctions

As I have demonstrated, FRET occurs between the Venus- and Cerulean-TS25-based-Ncad constructs when they are expressed either both in the same cell, or separately in adjacent cells, indicating that the same FRET pair can be used to detect both *cis* and *trans* interactions. This is not something that would necessarily be expected and may offer hints as to the geometry of cadherin molecules in an intact cell junction. It is not likely that FRET acceptor and donor fusions with EC2 would yield similar levels of FRET in both *cis* and *trans* experiments if the cadherin ectodomains were fully interdigitated, as in models proposed by Chappuis-Flament, Wong et al. (2001) and Sivasankar, Gumbiner et al. (2001). The distance between donor and acceptor displayed on EC2 would be expected to be shorter when donor- and acceptor-fusion cadherins are expressed on the same cell and considerably longer when the cadherin pair are expressed on adjacent cells, which would likely result in different levels of FRET (figure 12). As very similar levels of FRET were observed in my *cis* and *trans* interaction experiments, this model is not likely to be accurate.

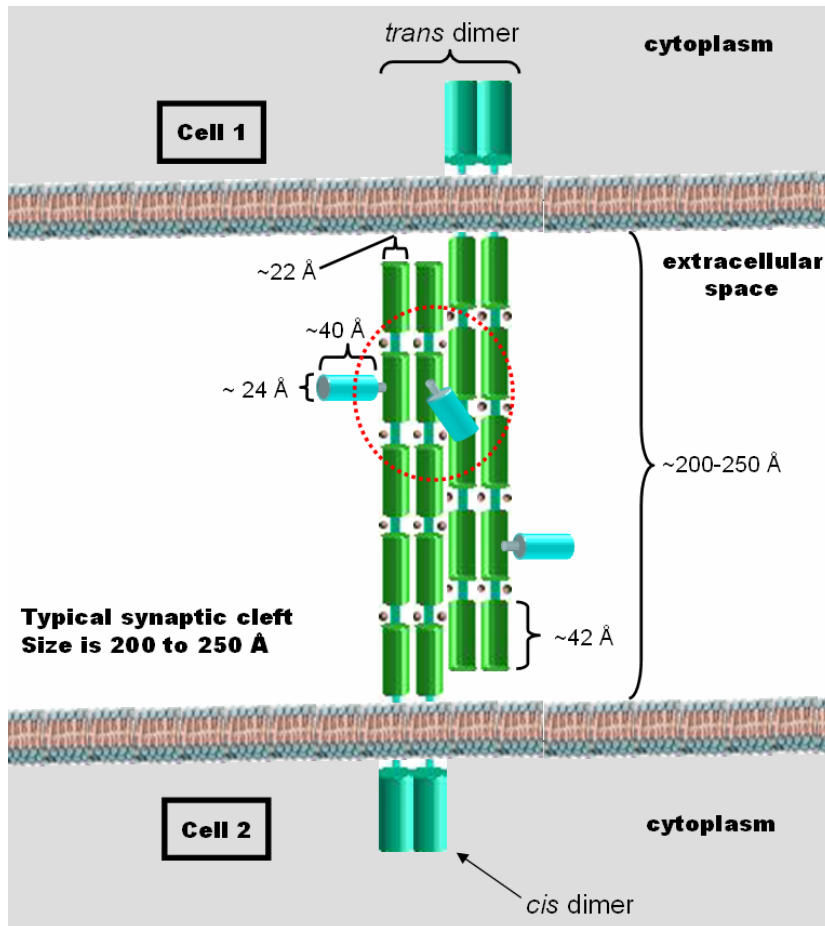


Figure 12. Quasi-to-scale schematic of fully interdigitated ectodomain model of cadherin interactions.

The symbols in the diagram represent the following: green cylinders, EC domains; brown circles, Ca^{2+} ions; blue cylinders, XFP FRET donor or acceptor fluorophores; grey cylinders, linker between XFP and cadherin created by transposon insertion. The dotted red circle represents the area within which FRET involving the circled XFP is expected to be strong.

However, if the models proposed by Boggon, (2002) and He, Cowin et al. (2003) were accurate, one might expect approximately similar levels of FRET in the *cis* and *trans* interaction experiments, as the distance between EC2s on both *cis* and *trans* interacting cadherins are approximately equivalent.

As an extension of this, it may be feasible to attempt to map the architecture of the cadherin interaction in intact cells through the combinatorial application of a small library of multiple FRET pairs with differing XFP insertion sites. As discussed in chapter IV, a single round of XFP insertion and selection yielded multiple viable insertion sites. It may be possible to repeat this process and obtain further cadherin-XFP fusions that would provide thorough coverage of the entire ectodomain (it also may be that, as no clones were obtained with insertions in the EC3-EC5 region, the Tn5-mediated insertion process is not entirely random and may be unable to create insertions in this region). If sufficient coverage of the ectodomain was obtained, the FRET levels of different combinations of XFP-fusions could be compared in both *cis* and *trans* experiments and used to generate a FRET efficiency “map” of the cadherin interaction.

Visualizing changes in cadherin-cadherin interactions induced by synaptic activity

As discussed, the motivation for undertaking this work was the observation that cadherins were present in hippocampal synapses and involved in plasticity, with functional cadherin adhesion being necessary for LTP (Tang, Hung et al. 1998). Now that proof-of-principle experiments have proved positive in heterologous cells, the next step is the neuronal expression of the FRET reporters. Transient transfection of hippocampal neurons can be done with calcium phosphate as well as lipid-based transfection methods (such as lipofectamine), but neither method are likely to yield a high enough efficiency to conduct *trans* interaction FRET experiments. I have tested transfection efficiency by lipofectamine 2000 and was able to transfect cultured neurons with the Venus-cadherin fusion protein (figure 13), but efficiency was very low (on the

order of one neuron per 35 mm dish). A more efficient method of delivering DNA will have to be used for neuronal experiments.

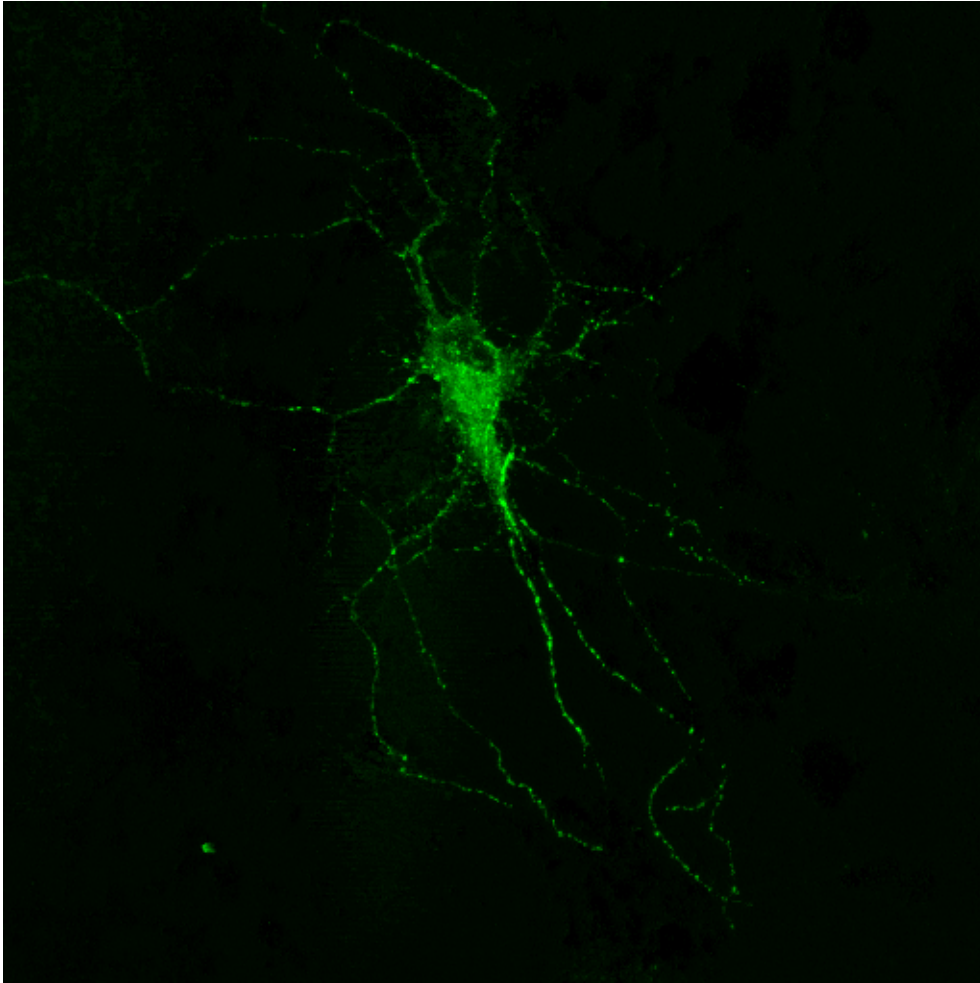


Figure 13. A hippocampal neuron expressing Venus-cadherin. Cultured hippocampal neurons (12 DIV) were transfected with Venus-cadherin fusion construct. The image was taken 30 hours after transfection.

Several possible methods are currently being explored: the use of biolistics, and viral infection. Once expression of the pair of FRET reporter constructs has been achieved in synaptically connected cells, one can begin to examine how activity regulates cadherin interactions.

Some consideration of the feasibility of detecting FRET signal changes at the synapse:

Spacek and Harris found puncta adherentia (PAs) at the edges of synapses on 33% of dendritic spines. The areas occupied by PAs were variable across different types of synapses, occupying $0.010 \pm 0.005 \mu\text{m}^2$ at macular synapses and $0.034 \pm 0.031 \mu\text{m}^2$ at perforated synapses (Spacek and Harris 1998). Based on electron tomographic data, C-cadherins are estimated to be present in desmosomes from neonatal mouse epidermis at a density of $\sim 17,000/\mu\text{m}^2$ (He et al. 2003). Assuming N-cadherin is present at the same density in neuronal puncta adherentia as C-cadherin is in epithelial desmosomes, this yields an estimate of 85–255 cadherins at a single macular synapse, and 51–1105 cadherins at a single perforated synapse. This estimate also assumes that N-cadherin is only present at puncta adherentia, and is not expressed synaptically outside of PAs.

This, of course, is an estimate of the numbers of endogenous cadherins present at a single hippocampal synapse. It is possible that overexpression of an XFP-fusion cadherin may be able to push more cadherins into the synapse, although the cell may have a compensatory mechanism by which it might regulate the number of cadherins at a synapse regardless of overexpression.

Because the FRET signal is generated by exogenously transfected fluorescent fusion proteins, overexpressed over a background of endogenous cadherins, not every cadherin present in the synapse will be displaying a FRET-capable fluorophore. This will result in lower FRET signal than a cell junction expressing only fusion cadherins. However, my experiments in HEK-293 and COS7 cells were also done in the presence of

endogenous cadherins - HEK-293 and COS7 cells both express high levels of endogenous cadherins, so it is not likely that neuronal expression will exact a further penalty on the FRET signal due to cadherin background. It has also been shown that overexpression of dominant negative cadherin mutants causes the down-regulation of endogenous cadherins (Norvell and Green 1998; Nieman, Kim et al. 1999; Troxell, Chen et al. 1999). It has been indicated that the β -catenin binding domain on the mutant cadherin was required for this (Norvell and Green 1998; Troxell, Chen et al. 1999). It is possible that overexpressing the FRET fusion constructs (which, though they do not act as dominant negatives, do have intact β -catenin binding domains) could cause both heterologous cells lines and neurons to compensate by down-regulating endogenous cadherin expression.

Synaptic activity can be manipulated in many ways; when expression of a pair of FRET reporter constructs has been achieved the following protocols should be considered:

- i) depolarization with KCl;
- ii) application of the neurotransmitter agonists AMPA or NMDA;
- iii) application of the GABA_A receptor antagonist bicuculline (by blocking fast inhibitory transmission, bicuculline increases action potential firing and thus promotes release of endogenous transmitter at synaptic sites);

- iv) application of antagonists that block excitatory synaptic transmission and action potential-dependent release (TTX, APV and CNQX cocktail);
- v) electrical stimulation, which promotes the release of synaptic transmitter and also allows for flexibility in the rates and frequencies of stimulation which may produce different effects on cadherin interactions at synaptic junctions.

When combined, these techniques should yield a wealth of new information about how different activity patterns may alter the strength of cadherin associations.

Experiments made possible with cadherin FRET reporters

I'd like to describe some of the unanswered questions regarding the role of cadherins in the synapse we should be able to use these constructs to address. By expressing the constructs in hippocampal slices we can take advantage of the well-established paradigm of hippocampal LTP. We should be able to achieve expression in slices by using Sindbis or Lenti viral vectors to infect cells in areas CA1 and/or CA3. Our laboratory has in the past achieved specific expression of exogenous DNA in these subsets of hippocampal cells through the use of stereotaxic injections of viral vectors into the hippocampus of live rats, specifically targeting CA1 or CA3.

One outstanding question is whether the Cadherin EC domain might be functioning as a synaptic cleft- Ca^{2+} sensor to detect synaptic transmission. To test this we can express the constructs in hippocampal slices and induce LTP. By monitoring FRET at the synapses formed by CA3 cells onto the CA1 cells, we can follow changes in cadherin adhesion in response to the synaptic activity induced by a single test pulse as well as during the high frequency tetanic stimulation used to induce LTP. Such a tetanus would be expected to cause a significant depletion of Ca^{2+} in the synaptic cleft, so we would expect to see a transient loss of cadherin adhesion during the tetanus, but would predict that no changes in cadherin adhesion would be observed during the single test pulses, as these were insufficient to allow for HAV peptide binding in Lixin's work (Tang, Hung et al. 1998).

Images can be taken at a temporal resolution on the order of milliseconds through line scans on a confocal microscope, or potentially using the higher speed made possible by a spinning (Nipkow) disk confocal microscope. This will allow us to capture cadherin interactions during these synaptic events.

We can also test the hypothesis that an increase in cadherin interactions contributes to an increase in synaptic strength. If this is true, we expect to measure an increase in cadherin adhesion after inducing potentiation. If we monitor FRET at CA3 -> CA1 synapses, this should be detected as an increase in FRET signal following LTP induction.

We can take advantage of the architecture of the hippocampus and the spatial resolution granted by imaging to confirm that observed changes in adhesion are the result of the strengthening of a specific synapse. If we express FRET reporter constructs in

CA1, CA3 and entorhinal cortex cells, we can selective potentiate either the CA3 or entorhinal cortex inputs to the CA1 cells and monitor the FRET signal at both sets of synapses. This gives us a within-cell control to verify if changes in adhesion are synapse-specific.

We can target donor and acceptor constructs to pre- and post-synaptic neurons to distinguish between *cis* and *trans* interactions. To monitor *trans* interactions, we can, for example, express one of the pair in CA1 cells and the other in CA3 cells. To monitor *cis* interactions we can express both donor and acceptor cadherins in a single population of cells, for example the CA1 cells and not transfect the CA3 cells. By doing this, we should be able to monitor a loss of cadherin *cis*-interactions independently of *trans*-interactions.

It is unknown exactly the degree to which extracellular calcium concentrations are lowered by synaptic activity. As it is known that as calcium concentrations are lowered, the *trans* interactions are the first to be lost and *cis* interactions require a larger decrease in calcium concentrations, we can use this technique to determine if a loss of *cis* interactions ever occurs, and during which types of synaptic activity.

In addition to a potential role for N-cadherin in synaptic plasticity, N-cadherin best known for its role in axon targeting. It has been demonstrated by convergent evidence from vertebrate and invertebrate systems that axons of neurons expressing N-cadherin mutants cannot migrate normally to their targets. More recently, it has been demonstrated that N-cadherin also plays a role in dendritic branching. The generally accepted idea, although it has not been decisively demonstrated, is that cadherin - cadherin interactions play a key role in forming appropriate synaptic connections. If we

assume that this is the case, then an outstanding question is how N-cadherin function can be restricted to specific sets of axon-target connections? Since N-cadherin is expressed ubiquitously throughout the visual system, how do the neurons avoid forming a giant mass of cell-cell adhesions? One idea is that N-cadherin activity is controlled spatiotemporally and functions when necessary at different points in development. For example, in neural development, axons of a particular cell type often extend together in a bundle and when they reach their general target location, they branch off to make specific contacts. A general target location is often segregated into cell populations that develop at different time windows. One hypothesis is that perhaps N-cadherin is not expressed at the membrane until a time window at which a given set of neurons is ready to form connections. This is difficult to examine using typical imaging methods because it is impossible to distinguish when cadherins are interacting.

We could use the FRET constructs here to determine at what point in development a cell begins to express “functional” or adhesive cadherins.

As a final note, I’d like to add that, although I’ve spotlighted the role of N-cadherin in neural systems, it is also expressed in cardiac and skeletal muscle tissue, and it plays a prominent role in cell adhesion, differentiation, embryogenesis, invasion, and signaling. Undoubtedly, these FRET constructs will provide a resource to understand the role of cadherin-cadherin interactions in wide variety of cell processes.

We now have the tools in hand to monitor cadherin adhesion in active synapses, which should provide further insight into the role of cadherins in plasticity and a wide variety of cellular processes.

WORK CITED

- Aakalu, G., W. B. Smith, et al. (2001). "Dynamic visualization of local protein synthesis in hippocampal neurons." Neuron **30**(2): 489-502.
- Anderson, P. and T. Lomo (1966). "Mode of activation of hippocampal pyramidal cells by excitatory synapses on dendrites." Exp Brain Res **2**(3): 247-60.
- Angst, B. D., C. Marcozzi, et al. (2001). "The cadherin superfamily." J Cell Sci **114**(Pt 4): 625-6
- Antonova, I., O. Arancio, et al. (2001). "Rapid increase in clusters of presynaptic proteins at onset of long-lasting potentiation." Science **294**(5546): 1547-50.
- Arndt, K., S. Nakagawa, et al. (1998). "Cadherin-defined segments and parasagittal cell ribbons in the developing chicken cerebellum." Mol Cell Neurosci **10**(5/6): 211-28.
- Bailey, C. H., D. Bartsch, et al. (1996). "Toward a molecular definition of long-term memory storage." Proc Natl Acad Sci U S A **93**(24): 13445-52.
- Baki, L., P. Marambaud, et al. (2001). "Presenilin-1 binds cytoplasmic epithelial cadherin, inhibits cadherin/p120 association, and regulates stability and function of the cadherin/catenin adhesion complex." Proc Natl Acad Sci U S A **98**(5): 2381-6.
- Bamji, S. X., B. Rico, et al. (2006). "BDNF mobilizes synaptic vesicles and enhances synapse formation by disrupting cadherin-beta-catenin interactions." J Cell Biol **174**(2): 289-99.
- Bamji, S. X., K. Shimazu, et al. (2003). "Role of beta-catenin in synaptic vesicle localization and presynaptic assembly." Neuron **40**(4): 719-31.
- Beesley, P. W., R. Mummery, et al. (1995). "N-cadherin is a major glycoprotein component of isolated rat forebrain postsynaptic densities." J Neurochem **64**(5): 2288-94.
- Benson, D. L. and H. Tanaka (1998). "N-cadherin redistribution during synaptogenesis in hippocampal neurons." J Neurosci **18**(17): 6892-904.
- Blaschuk, O. W., R. Sullivan, et al. (1990). "Identification of a cadherin cell adhesion recognition sequence." Dev Biol **139**(1): 227-9.
- Bliss, T. V. and G. L. Collingridge (1993). "A synaptic model of memory: long-term potentiation in the hippocampus." Nature **361**(6407): 31-9.

- Bliss, T. V. and T. Lomo (1973). "Long-lasting potentiation of synaptic transmission in the dentate area of the anaesthetized rabbit following stimulation of the perforant path." J Physiol **232**(2): 331-56.
- Boggon, T. J., J. Murray, et al. (2002). "C-cadherin ectodomain structure and implications for cell adhesion mechanisms." Science **296**(5571): 1308-13.
- Bozdagi, O., W. Shan, et al. (2000). "Increasing numbers of synaptic puncta during late-phase LTP: N-cadherin is synthesized, recruited to synaptic sites, and required for potentiation." Neuron **28**(1): 245-59.
- Bozdagi, O., M. Valcin, et al. (2004). "Temporally distinct demands for classic cadherins in synapse formation and maturation." Mol Cell Neurosci **27**(4): 509-21.
- Brembeck, F. H., M. Rosario, et al. (2006). "Balancing cell adhesion and Wnt signaling, the key role of beta-catenin." Curr Opin Genet Dev **16**(1): 51-9.
- Broudy, V. C., N. L. Lin, et al. (1998). "Analysis of c-kit receptor dimerization by fluorescence resonance energy transfer." Blood **91**(3): 898-906.
- Buchs, P. A. and D. Muller (1996). "Induction of long-term potentiation is associated with major ultrastructural changes of activated synapses." Proc Natl Acad Sci USA **93**(15): 8040-5.
- Chappuis-Flament, S., E. Wong, et al. (2001). "Multiple cadherin extracellular repeats mediate homophilic binding and adhesion." J Cell Biol **154**(1): 231-43.
- Cho, K. O., C. A. Hunt, et al. (1992). "The rat brain postsynaptic density fraction contains a homolog of the Drosophila discs-large tumor suppressor protein." Neuron **9**(5): 929-42.
- Damjanovich, S., L. Bene, et al. (1997). "Preassembly of interleukin 2 (IL-2) receptor subunits on resting Kit 225 K6 T cells and their modulation by IL-2, IL-7, and IL-15: a fluorescence resonance energy transfer study." Proc Natl Acad Sci USA **94**(24): 13134-9.
- Egelman, D. M. and P. R. Montague (1998). "Computational properties of peri-dendritic calcium fluctuations." J Neurosci **18**(21): 8580-9.
- Egelman, D. M. and P. R. Montague (1999). "Calcium dynamics in the extracellular space of mammalian neural tissue." Biophys J **76**(4): 1856-67.
- Engert, F. and T. Bonhoeffer (1999). "Dendritic spine changes associated with hippocampal long-term synaptic plasticity." Nature **399**(6731): 66-70.

- Fannon, A. M. and D. R. Colman (1996). "A model for central synaptic junctional complex formation based on the differential adhesive specificities of the cadherins." Neuron **17**(3): 423-34.
- Guo, C., S. K. Dower, et al. (1995). "Fluorescence resonance energy transfer reveals interleukin (IL)-1-dependent aggregation of IL-1 type I receptors that correlates with receptor activation." J Biol Chem **270**(46): 27562-8.
- He, W., P. Cowin, et al. (2003). "Untangling desmosomal knots with electron tomography." Science **302**(5642): 109-13.
- Huntley, G. W. and D. L. Benson (1999). "Neural (N)-cadherin at developing thalamocortical synapses provides an adhesion mechanism for the formation of somatopically organized connections." J Comp Neurol **407**(4): 453-71.
- Hyafil, F., C. Babinet, et al. (1981). "Cell-cell interactions in early embryogenesis: A molecular approach to the role of calcium." Cell **26**(3 Pt 1): 447-54.
- Inoue, A. and J. R. Sanes (1997). "Lamina-specific connectivity in the brain: Regulation by N-cadherin, neurotrophins, and glycoconjugates." Science **276**(5317): 1428-31.
- Jones, R. S. and U. H. Heinemann (1987). "Differential effects of calcium entry blockers on pre- and postsynaptic influx of calcium in the rat hippocampus in vitro." Brain Res **416**(2): 257-66.
- Kenworthy, A. K. and M. Edidin (1998). "Distribution of a glycosylphosphatidylinositol-anchored protein at the apical surface of MDCK cells examined at a resolution of <100 Å using imaging fluorescence resonance energy transfer." J Cell Biol **142**(1): 69-84.
- Kenworthy, A. K., N. Petranova, et al. (2000). "High-resolution FRET microscopy of cholera toxin B-subunit and GPI-anchored proteins in cell plasma membranes." Mol Biol Cell **11**(5): 1645-55.
- Koch, A. W., S. Pokutta, et al. (1997). "Calcium binding and homoassociation of E-cadherin domains." Biochemistry **36**(25): 7697-705.
- Maletic-Savatic, M., R. Malinow, et al. (1999). "Rapid dendritic morphogenesis in CA1 hippocampal dendrites induced by synaptic activity." Science **283**(5409): 1923-7.
- Muller, T., A. Choidas, et al. (1999). "Phosphorylation and free pool of beta-catenin are regulated by tyrosine kinases and tyrosine phosphatases during epithelial cell migration." J Biol Chem **274**(15): 10173-83.

- Murase, S., E. Mosser, et al. (2002). "Depolarization drives beta-Catenin into neuronal spines promoting changes in synaptic structure and function." Neuron **35**(1): 91-105.
- Nagafuchi, A., Y. Shirayoshi, et al. (1987). "Transformation of cell adhesion properties by exogenously introduced E-cadherin cDNA." Nature **329**(6137): 341-3.
- Nagafuchi, A. and M. Takeichi (1988). "Cell binding function of E-cadherin is regulated by the cytoplasmic domain." Embo J **7**(12): 3679-84.
- Nagai, T. K. Ibata, et al. (2002). "A variant of yellow fluorescent protein with fast and efficient maturation for cell-biological applications." Nat Biotechnol **20**(1): 87-90.
- Nagar, B., M. Overduin, et al. (1996). "Structural basis of calcium-induced E-cadherin rigidification and dimerization." Nature **380**(6572): 360-4.
- Nicoll, R. A. and R. C. Malenka (1999). "Expression mechanisms underlying NMDA receptor-dependent long-term potentiation." Ann N Y Acad Sci **868**: 515-25.
- Nieman, M. T., J. B. Kim, et al. (1999). "Mechanism of extracellular domain-deleted dominant negative cadherins." J Cell Sci **112 (Pt 10)**: 1621-32.
- Norvell, S. M. and K. J. Green (1998). "Contributions of extracellular and intracellular domains of full length and chimeric cadherin molecules to junction assembly in epithelial cells." J Cell Sci **111 (Pt 9)**: 1305-18.
- Nose, A., K. Tsuji, et al. (1990). "Localization of specificity determining sites in cadherin cell adhesion molecules." Cell **61**(1): 147-55.
- Overduin, M., T. S. Harvey, et al. (1995). "Solution structure of the epithelial cadherin domain responsible for selective cell adhesion." Science **267**(5196): 386-9.
- Ozawa, M. and R. Kemler (1990). "Correct proteolytic cleavage is required for the cell adhesive function of uvomorulin." J Cell Biol **111**(4): 1645-50.
- Pasdar, M., K. A. Krzeminski, et al. (1991). "Regulation of desmosome assembly in MDCK epithelial cells: Coordination of membrane core and cytoplasmic plaque domain assembly at the plasma membrane." J Cell Biol **113**(3): 645-55.
- Pathre, P., C. Arregui, et al. (2001). "PTP1B regulates neurite extension mediated by cell-cell and cell-matrix adhesion molecules." J Neurosci Res **63**(2): 143-50.
- Perret, E., A. M. Benoliel, et al. (2002). "Fast dissociation kinetics between individual E-cadherin fragments revealed by flow chamber analysis." Embo J **21**(11): 2537-46.

- Perret, E., A. Leung, et al. (2004). "Trans-bonded pairs of E-cadherin exhibit a remarkable hierarchy of mechanical strengths." Proc Natl Acad Sci USA **101**(47): 16472-7.
- Pertz, O., D. Bozic, et al. (1999). "A new crystal structure, Ca²⁺ dependence and mutational analysis reveal molecular details of E-cadherin homoassociation." Embo J **18**(7): 1738-47.
- Pokutta, S., K. Herrenknecht, et al. (1994). "Conformational changes of the recombinant extracellular domain of E-cadherin upon calcium binding." Eur J Biochem **223**(3): 1019-26.
- Posthaus, H., C. M. Dubois, et al. (1998). "Proprotein cleavage of E-cadherin by furin in baculovirus over-expression system: potential role of other convertases in mammalian cells." FEBS Lett **438**(3): 306-10.
- Posthaus, H., C. M. Dubois, et al. (2003). "Novel insights into cadherin processing by subtilisin-like convertases." FEBS Lett **536**(1-3): 203-8.
- Rizzo, M. A., G. H. Springer, et al. (2004). "An improved cyan fluorescent protein variant useful for FRET." Nat Biotechnol **22**(4): 445-9.
- Roura, S., S. Miravet, et al. (1999). "Regulation of E-cadherin/Catenin association by tyrosine phosphorylation." J Biol Chem **274**(51): 36734-40.
- Rusakov, D. A. and A. Fine (2003). "Extracellular Ca²⁺ depletion contributes to fast activity-dependent modulation of synaptic transmission in the brain." Neuron **37**(2): 287-97.
- Rusakov, D. A. and D. M. Kullmann (1998). "Geometric and viscous components of the tortuosity of the extracellular space in the brain." Proc Natl Acad Sci USA **95**(15): 8975-80.
- Schikorski, T. and C. F. Stevens (1997). "Quantitative ultrastructural analysis of hippocampal excitatory synapses." J Neurosci **17**(15): 5858-67.
- Schuman, E. M. and S. Murase (2003). "Cadherins and synaptic plasticity: activity-dependent cyclin-dependent kinase 5 regulation of synaptic beta-catenin-cadherin interactions." Philos Trans R Soc Lond B Biol Sci **358**(1432): 749-56.
- Selvin, P. R. (1995). "Fluorescence resonance energy transfer." Methods Enzymol **246**: 300-34.
- Shapiro, L., A. M. Fannon, et al. (1995). "Structural basis of cell-cell adhesion by cadherins." Nature **374**(6520): 327-37.

- Shepherd, G. M. and K. M. Harris (1998). "Three-dimensional structure and composition of CA3-->CA1 axons in rat hippocampal slices: implications for presynaptic connectivity and compartmentalization." J Neurosci **18**(20): 8300-10.
- Sivasankar, S., B. Gumbiner, et al. (2001). "Direct measurements of multiple adhesive alignments and unbinding trajectories between cadherin extracellular domains." Biophys J **80**(4): 1758-68.
- Sommers, C. L., E. P. Gelmann, et al. (1994). "Alterations in beta-catenin phosphorylation and plakoglobin expression in human breast cancer cells." Cancer Res **54**(13): 3544-52.
- Sorkin, A., M. McClure, et al. (2000). "Interaction of EGF receptor and grb2 in living cells visualized by fluorescence resonance energy transfer (FRET) microscopy." Curr Biol **10**(21): 1395-8.
- Spacek, J. and K. M. Harris (1998). "Three-dimensional organization of cell adhesion junctions at synapses and dendritic spines in area CA1 of the rat hippocampus." J Comp Neurol **393**(1): 58-68.
- Sperry, R. W. (1963). "Chemoaffinity in the orderly growth of nerve fiber patterns and connections." Proc Natl Acad Sci USA **50**: 703-10.
- Suzuki, S. T. (1996). "Protocadherins and diversity of the cadherin superfamily." J Cell Sci **109** (Pt 11): 2609-11.
- Takeichi, M. and K. Abe (2005). "Synaptic contact dynamics controlled by cadherin and catenins." Trends Cell Biol **15**(4): 216-21.
- Tamura, K., W. S. Shan, et al. (1998). "Structure-function analysis of cell adhesion by neural (N-) cadherin." Neuron **20**(6): 1153-63.
- Tanaka, H., W. Shan, et al. (2000). "Molecular modification of N-cadherin in response to synaptic activity." Neuron **25**(1): 93-107.
- Tang, L., C. P. Hung, et al. (1998). "A role for the cadherin family of cell adhesion molecules in hippocampal long-term potentiation." Neuron **20**(6): 1165-75.
- Togashi, H., K. Abe, et al. (2002). "Cadherin regulates dendritic spine morphogenesis." Neuron **35**(1): 77-89.
- Troxell, M. L., Y. T. Chen, et al. (1999). "Cadherin function in junctional complex rearrangement and posttranslational control of cadherin expression." Am J Physiol **276**(2 Pt 1): C404-18.

- Uchida, N., Y. Honjo, et al. (1996). "The catenin/cadherin adhesion system is localized in synaptic junctions bordering transmitter release zones." J Cell Biol **135**(3): 767-79.
- Wheeler, G. N., A. E. Parker, et al. (1991). "Desmosomal glycoprotein DGI, a component of intercellular desmosome junctions, is related to the cadherin family of cell adhesion molecules." Proc Natl Acad Sci USA **88**(11): 4796-800.
- Wiest, M. C., D. M. Eagleman, et al. (2000). "Dendritic spikes and their influence on extracellular calcium signaling." J Neurophysiol **83**(3): 1329-37.
- Yagi, T. and M. Takeichi (2000). "Cadherin superfamily genes: Functions, genomic organization, and neurologic diversity." Genes Dev **14**(10): 1169-80.
- Yap, A. S., C. M. Niessen, et al. (1998). "The juxtamembrane region of the cadherin cytoplasmic tail supports lateral clustering, adhesive strengthening, and interaction with p120ctn." J Cell Biol **141**(3): 779-89.
- Yuste, R. and T. Bonhoeffer (2004). "Genesis of dendritic spines: Insights from ultrastructural and imaging studies." Nat Rev Neurosci **5**(1): 24-34.
- Zhu, B., S. Chappuis-Flament, et al. (2003). "Functional analysis of the structural basis of homophilic cadherin adhesion." Biophys J **84**(6): 4033-42.

APPENDIX

MATERIALS AND METHODS

Constructs, viruses and antibodies

Mouse N-cadherin cDNA in a mammalian expression vector (pCXN2-Ncad) was provided by Dr. Deanna Benson. To enhanced the surface expression level of N-cadherin, the construct was modified by adding a Kozak sequence in front of the start codon of N-cadherin protein and moving the entire cDNA into a different expression vector, pcDNA3.1Zeo(-)(Invitrogen). All PCR-modified constructs have been confirmed by DNA sequencing. Anti-GFP and β -catenin antibodies are purchased from Molecular Probes and Zymed respectively. Transfection and Sindbis virus infection were performed as described previously (Aakalu, 2001).

Cultured hippocampal neurons

Dissociated hippocampal neurons were prepared and maintained as previously described (Aakalu, 2001). Briefly, hippocampi from postnatal day 2 Sprague-Dawley rat pups were enzymatically and mechanically dissociated and plated into poly-lysine coated glass-bottom petri dishes (Mattek). Neurons were maintained for 14-21 days at 37° C in growth medium (Neurobasal A supplemented with B27 and Glutamax-1, Invitrogen).

Cell culture and transfection

L, HEK293, and COS-7 cells were grown in Dulbecco's modified Eagle's medium with 10% fetal bovine serum and penicillin/streptomycin (Invitrogen). For transient transfection, cells were plated either in a Mattek dish for microscopy or in a 35 mm culture dish for immunoprecipitation, grown to 80% to 90% confluence, then transfected with the appropriate amount of DNA mixed with lipofectAMINE (Invitrogen). Transient expression was allowed for 40 to 48 hours. To generate stable lines, L cells were plated into 10 cm culture dishes and transfected with 10 µg of DNA (TS25 with either the YFP or CFP insertions) with LipofectAMINE (Invitrogen). After 48 hours of transient expression, 500 µg/mL of Geneticin (Invitrogen) was added into the medium. Fresh Geneticin-containing media was supplemented every day for 10 days until visible colonies were observed under the microscope. Twenty-four colonies of each construct were amplified sequentially through a series of clonal expansions from 96-well plate to 24-well plate. In preliminary experiments, ten clones survived and were analyzed by immunoblotting using an anti-GFP antibody.

Immunoprecipitation

COS-7 cells were transfected with plasmid DNA purified from either Maxiprep or QIAprep spin miniprep kits (Qiagen) with LipofectAMINE reagents overnight at 37°C. Forty-eight hours after the addition of the DNA/liposome mixture, cells were washed three times with ice-cold PBS-MC (phosphate buffered saline, 1 mM MgCl₂, 0.1 mM

CaCl₂) and lysed with NP40 lysis buffer (1% NP40, 150 mM NaCl, 50 mM Tris HCl pH 8.0) with freshly added protease inhibitor cocktail (Roche). Cells were incubated on ice for 20 minutes and spin at 13,000 rpm for 15 minutes at 4°C in a microfuge. The centrifuged extracts were then mixed with lysis buffer-washed Protein G beads (Pierce) and incubated at 4°C overnight with gentle rotation. Beads were washed three times with the lysis buffer at room temperature for 10 minutes each and boiled in 5X SDS-PAGE sample buffer for 5 minutes. The entire eluate with 2% of the supernatant were loaded into 5%-15% SDS-polyacrylamide gel and transferred onto PVDF membrane (BioRad). Immunoblotting was performed with various antibodies against tags or specific proteins.

L cell aggregation assay

Stable lines were plated into 35 mm dishes until 80% to 90% confluent. All dishes were washed three times with prewarmed PBS+1mM CaCl₂, then incubated with 500 mL of 0.01% trypsin in PBS + 1 mM CaCl₂ at 37°C for 30 minutes. The trypsinized cell suspensions were transferred into microfuge tubes and centrifuged at 1,000 rpm at room temperature for 5 minutes. The pelleted cells were washed twice with equal volumes of PBS + 1% BSA. The cell suspension was then divided into two tubes containing PBS + 1% BSA with or without 5 mM CaCl₂, and incubated at 37°C for 1 hour with head-to-tail rotation. The contents of the tubes were plated into 35 mm dishes and cell aggregates are observed under the microscope.

Microscopy and image analysis

All images were acquired with a Zeiss 510 Meta confocal laser scanning microscope. YFP is excited with the 514 nm line of an argon ion laser using a Plan-Neofluor IR 40X 1.3 NA oil immersion objective (Zeiss), and emitted light was collected over a spectrum of wavelengths between 462 and 633 nm with bandwidths of 10.7 nm. CFP was excited with the 458 nm line of a argon ion laser, and emitted light was collected over the same spectrum of wavelengths used for YFP detection. Because there is significant overlap in the emission spectra of YFP and CFP, the fluorescence contribution of each fluorophore at each pixel was separated using a linear unmixing algorithm based on the spectral signatures of YFP and CFP created from reference lambda stack images of cells expressing either soluble YFP or soluble CFP, respectively. Between-dish comparisons on a given day, all images were acquired at the same settings, without knowledge of the experimental condition during image acquisition. All postacquisition processing and analysis was carried out with ImageJ (NIH) and Matlab (The MathWorks, Inc.).